

Quantum-geometry-induced anapole superconductivity

Taisei Kitamura,^{1,*} Shota Kanasugi,¹ Michiya Chazono,¹ and Youichi Yanase¹

¹*Department of Physics, Graduate School of Science, Kyoto University, Kyoto 606-8502, Japan*

(Dated: March 24, 2023)

Anapole superconductivity recently proposed for multiband superconductors [Commun. Phys. 5, 39 (2022)] is a key feature of time-reversal (\mathcal{T})-symmetry-broken polar superconductors. The anapole moment was shown to arise from the asymmetric Bogoliubov spectrum, which induces a finite center of mass momenta of Cooper pairs at the zero magnetic field. In this paper, we show an alternative mechanism of anapole superconductivity: the quantum geometry induces the anapole moment when the interband pairing and Berry connection are finite. Thus, the anapole superconductivity is a ubiquitous feature of \mathcal{T} -broken multiband polar superconductors. Applying the theory to a minimal model of UTe_2 , we demonstrate the quantum-geometry-induced anapole superconductivity. Furthermore, we show the Bogoliubov Fermi surfaces (BFS) in an anapole superconducting state and predict an unusual temperature dependence of BFS due to the quantum geometry. Experimental verification of these phenomena may clarify the superconducting state in UTe_2 and reveal the ubiquitous importance of quantum geometry in exotic superconductors.

I. INTRODUCTION

Parity-mixed superconductors, in which even- and odd-parity pairings coexist, are attracting much attention, as the parity-mixing phenomena are closely related to the space inversion (\mathcal{P})-symmetry breaking. Stimulated by the discovery of noncentrosymmetric superconductivity in heavy fermions and artificial heterostructures, time-reversal (\mathcal{T})-symmetric parity-mixed pairing states such as the $s + p$ -wave state have been investigated intensively^{1,2}. For a long time, studies focused on the crystals lacking the \mathcal{P} -symmetry allowing an antisymmetric spin-orbit coupling (ASOC). Consequently, the Rashba superconductor and the Ising superconductor have become fundamental concepts in condensed matter physics^{1,2}.

On the other hand, centrosymmetric crystals were recently shown to be an intriguing platform of spontaneously \mathcal{P} -symmetry breaking superconductivity³⁻⁵. In the absence of the ASOC, additional \mathcal{T} -symmetry breaking is expected³⁻⁵ as the $\pm\pi/2$ phase difference between even- and odd-parity pairing potentials, such as the $s + ip$ -wave pairing state, is energetically favored. As a result, both of the \mathcal{P} - and \mathcal{T} -symmetry are broken while the combined \mathcal{PT} -symmetry is preserved. The three-dimensional $s + ip$ -wave pairing state in single-band superconductors was theoretically studied as a superconducting analog⁶⁻⁸ of axion insulators^{9,10}. Such a pairing state in Sr_2RuO_4 was theoretically proposed¹¹. Furthermore, recently discovered candidate for spin-triplet superconductor UTe_2 ^{12,13} is predicted to realize the $s + ip$ -wave pairing state¹⁴, as it is consistent with the experimentally observed multiple superconducting phases¹⁵⁻²¹ and multiple magnetic fluctuations²²⁻²⁷.

Clarification of the \mathcal{PT} -symmetric parity-mixed superconductivity has been awaited to uncover an exotic state of matter. However, properties of the \mathcal{PT} -symmetric parity-mixed superconductivity are almost unresolved. In particular, theoretical studies of *multiband* superconductors have not been carried out except for Ref. 28, although it is known that intriguing superconducting phenomena such as the intrinsic polar Kerr effect²⁹⁻³¹ and Bogoliubov Fermi surfaces (BFS)^{32,33} may appear from multiband properties. In Ref. 28, the anapole su-

perconductivity was discussed as an exotic feature of the \mathcal{PT} -symmetric parity-mixed pairing state in multiband superconductors. If some conditions are satisfied, an asymmetric Bogoliubov spectrum (BS) arises from the interband pairing²⁸. When the symmetry of superconductivity has a polar property, such as in the $A_g + iB_{3u}$ pairing state proposed for UTe_2 ¹⁴, the asymmetric BS induces an effective anapole moment, which is defined as the first-order coefficient of the free energy in terms of the center of mass momenta of Cooper pairs. The anapole moment characterizes the anapole superconductivity as it does the anapole order in magnetic materials³⁴⁻³⁸ and nucleus³⁹.

The anapole moment is a polar and \mathcal{T} -odd vector³⁴, which shares the symmetry as the velocity and momentum. Therefore, it is not surprising that the effective anapole moment induces a finite center of mass momenta of Cooper pairs \mathbf{q} even in the absence of the magnetic field. The mechanism of finite- \mathbf{q} pairing is different from the Fulde-Ferrell-Larkin-Ovchinnikov (FFLO) superconductivity^{40,41} and helical superconductivity^{1,2}, which require a finite magnetic field. In contrast to the FFLO and helical superconductivity, the anapole superconductivity can be studied with avoiding experimental difficulties due to vortices induced by an external magnetic field. For instance, the anapole domain switching²⁸, superconducting piezoelectric effect^{42,43}, and Josephson effect^{44,45} may uncover intrinsic properties of anapole superconductivity. Therefore, the anapole superconductivity may be the key to elucidating the \mathcal{PT} -symmetric parity-mixed pairing state, and it may realize and clarify the finite- \mathbf{q} pairing state which has been searched for a long time^{1,2,46}.

In this paper, we show that the anapole superconductivity is a ubiquitous feature more than revealed in the previous paper²⁸, considering the *quantum geometry* extensively studied in various fields^{37,38,47-58}. Recently, an essential role of the quantum geometry in the superfluid weight, namely, the second-order derivative of the free energy, has been revealed⁵⁹⁻⁶². Thus, it is naturally expected that the quantum geometry may be essential for the anapole superconductivity.

First, we provide a thorough formulation of the anapole moment based on the Bardeen-Cooper-Schrieffer (BCS) mean-field theory. The obtained formula contains two terms; one is

the geometric term and the other is the group velocity term. Only a part of the group velocity term was derived in the previous literature²⁸. Based on the general two-band model with Kramers degeneracy, the microscopic origin of the geometric term is revealed to be the interband pairing and the Berry connection, while the group velocity term is induced by the asymmetric BS. Then, applying the theory to a model of UTe₂, we demonstrate the quantum-geometry-induced anapole superconductivity. Moreover, we show unique features of anapole superconductivity. When the system has a small gap minimum as expected for UTe₂¹³, the anapole moment induces the BFS. The BFS may show a reappearing behavior as decreasing the temperature, causing anomalies in density of states (DOS) and thermodynamic quantities.

II. GENERAL FORMULA FOR ANAPOLE MOMENT

An order parameter of the anapole superconductivity is the anapole moment which is defined by the first-order coefficient of the free energy with respect to \mathbf{q} . In the previous study²⁸, the anapole moment is derived only when the \mathbf{k} -derivative of normal-state Hamiltonian is proportional to the identity matrix, namely, $\partial_\mu H_{\mathbf{k}} \propto \mathbf{1}$. We adopt the notation $\partial_\mu = \partial_{k_\mu}$, and $H_{\mathbf{k}}$ is the matrix representation of the single-particle Hamiltonian. Below, we formulate the anapole moment in the general case based on the BCS mean-field theory.

The normal state is assumed to be \mathcal{P} - and \mathcal{T} -symmetric, and therefore, $H_{\mathbf{k}} = U_{\mathcal{T}} H_{-\mathbf{k}}^T U_{\mathcal{T}}^\dagger$ is satisfied, where $U_{\mathcal{T}} = i\sigma_y \otimes \mathbf{1}$ is the unitary part of the \mathcal{T} operator with the Pauli matrix for the spin space σ_μ ($\mu = 0, x, y, z$). Thus, the Bogoliubov-de Gennes (BdG) Hamiltonian for a finite- \mathbf{q} pairing state can be written as (see Appendix A)

$$\hat{H}^{\text{BdG}} = \frac{1}{2} \sum_{\mathbf{k}} \hat{\Psi}_{\mathbf{k},\mathbf{q}}^\dagger H_{\mathbf{k},\mathbf{q}}^{\text{BdG}} \hat{\Psi}_{\mathbf{k},\mathbf{q}}, \quad (1)$$

$$H_{\mathbf{k},\mathbf{q}}^{\text{BdG}} = \begin{pmatrix} H_{\mathbf{k}+\mathbf{q}} & \Delta_{\mathbf{k}} \\ \Delta_{\mathbf{k}}^\dagger & -H_{\mathbf{k}-\mathbf{q}} \end{pmatrix}, \quad (2)$$

$$\hat{\Psi}_{\mathbf{k},\mathbf{q}}^\dagger = \left(\hat{c}_{\mathbf{k}+\mathbf{q}}^\dagger \quad \hat{c}_{-\mathbf{k}+\mathbf{q}}^T U_{\mathcal{T}}^\dagger \right). \quad (3)$$

Here, we denote $\hat{c}_{\mathbf{k}}^\dagger = (\hat{c}_{\uparrow 1\mathbf{k}}^\dagger \cdots \hat{c}_{\uparrow f\mathbf{k}}^\dagger \hat{c}_{\downarrow 1\mathbf{k}}^\dagger \cdots \hat{c}_{\downarrow f\mathbf{k}}^\dagger)$, where $\hat{c}_{\sigma l\mathbf{k}}^\dagger$ is the creation operator for spin σ and the other internal degree of freedom l . We consider general cases, including multi-orbital and multi-sublattice systems, and f is the total number of degrees of freedom other than spin.

The off-diagonal part $\Delta_{\mathbf{k}} = \Delta_{\mathbf{k}}^g + \Delta_{\mathbf{k}}^u$ is the gap function in the matrix representation, where $\Delta_{\mathbf{k}}^g$ is the \mathcal{P} -even (odd) component of the pair potential. Coexistence of Cooper pairs with different parities, i.e. parity-mixed state, leads to broken \mathcal{P} -symmetry. Furthermore, the \mathcal{T} -symmetry breaking is theoretically predicted³⁻⁵, when the normal state preserves the \mathcal{P} -symmetry. Thus, we assume the $\pm\pi/2$ phase difference between $\Delta_{\mathbf{k}}^g$ and $\Delta_{\mathbf{k}}^u$, consistent with the theoretical prediction³⁻⁵. As a result the \mathcal{P} - and \mathcal{T} -symmetry are broken by the parity-mixed gap function while the \mathcal{PT} -symmetry is preserved. In addition, to make the anapole moment finite,

throughout the paper, we assume the gap function $\Delta_{\mathbf{k}}$ belongs to polar irreducible representation.

Expanding the free energy by \mathbf{q} as $F_{\mathbf{q}} = T \cdot \mathbf{q} + \cdots$, we obtain the anapole moment as,

$$T_\mu = \frac{1}{2} \sum_{\mathbf{k}} \sum_a f(E_{a\mathbf{k}}) \langle \psi_{a\mathbf{k}} | \partial_\mu H_{\mathbf{k}}^+ | \psi_{a\mathbf{k}} \rangle, \quad (4)$$

$$H_{\mathbf{k}}^+ = \begin{pmatrix} H_{\mathbf{k}} & 0 \\ 0 & H_{\mathbf{k}} \end{pmatrix}. \quad (5)$$

Here, we use the eigenvalue equation $H_{\mathbf{k}}^{\text{BdG}} |\psi_{a\mathbf{k}}\rangle = E_{a\mathbf{k}} |\psi_{a\mathbf{k}}\rangle$ with $H_{\mathbf{k}}^{\text{BdG}} \equiv H_{\mathbf{k},0}^{\text{BdG}}$ and the Fermi-distribution function $f(E)$. The derivation of Eq. (4) is shown in Appendix A. When the anapole moment in superconductors T_μ is finite, a superconducting state due to Cooper pairs with finite center of mass momenta becomes most stable.

To obtain further insights, using the Bloch wave function which follows $H_{\mathbf{k}} |u_{n\chi\mathbf{k}}\rangle = \epsilon_{n\mathbf{k}} |u_{n\chi\mathbf{k}}\rangle$, we expand $|\psi_a(\mathbf{k})\rangle$ as $|\psi_a(\mathbf{k})\rangle = \left(\sum_{n,\chi} \phi_{n\chi\mathbf{k}}^{a+} |u_{n\chi\mathbf{k}}\rangle \sum_{n,\chi} \phi_{n\chi\mathbf{k}}^{a-} |u_{n\chi\mathbf{k}}\rangle \right)^T$. Because of Kramers degeneracy, we distinguish two degenerate bands by the helicity $\chi = \uparrow\downarrow$. Here, $\phi_{n\chi\mathbf{k}}^{\pm}$ is the matrix element of the unitary matrix which diagonalizes the band representation of the BdG Hamiltonian. After calculations, the anapole moment Eq. (4) is divided into two parts,

$$T_\mu = T_\mu^{\text{velo}} + T_\mu^{\text{geom}}, \quad (6)$$

where

$$T_\mu^{\text{velo}} = \sum_{\mathbf{k}} \sum_{n,\chi} C_{n\chi n\chi\mathbf{k}} \partial_\mu \epsilon_{n\mathbf{k}}, \quad (7)$$

$$T_\mu^{\text{geom}} = \sum_{\mathbf{k}} \sum_{n \neq m, \chi\chi'} C_{n\chi m\chi'\mathbf{k}} \times (\epsilon_{m\mathbf{k}} - \epsilon_{n\mathbf{k}}) \langle u_{n\chi\mathbf{k}} | \partial_\mu u_{m\chi'\mathbf{k}} \rangle, \quad (8)$$

$$C_{n\chi m\chi'\mathbf{k}} = \frac{1}{2} \sum_a f(E_{a\mathbf{k}}) \left(\phi_{n\chi\mathbf{k}}^{a+*} \phi_{m\chi'\mathbf{k}}^{a+} + \phi_{n\chi\mathbf{k}}^{a-*} \phi_{m\chi'\mathbf{k}}^{a-} \right). \quad (9)$$

T_μ^{velo} in Eq. (7) is called the group velocity term as it contains the group velocity $\partial_\mu \epsilon_{n\mathbf{k}}$. In the next section, using the general two-band model, we show that this term arises from the asymmetric BS. Equation (8) for T_μ^{geom} is named the geometric term because it contains the Berry connection $\langle u_{n\chi\mathbf{k}} | \partial_\mu u_{m\chi'\mathbf{k}} \rangle$. Through the Berry connection in the geometric term, the geometric properties of Bloch electrons may contribute to the anapole moment. Some conditions have to be satisfied for a finite group velocity term, which vanishes in simple models²⁸. On the other hand, the geometric term has been overlooked in the previous study. Owing to the geometric term, the anapole superconductivity becomes recognized as a ubiquitous feature of the \mathcal{PT} -symmetric mixed-parity pairing state in multiband superconductors.

III. ORIGIN OF ANAPOLE SUPERCONDUCTIVITY

A. General discussion

Before demonstrating the anapole superconductivity due to quantum geometry, we discuss the physical origin and the microscopic process of the anapole moment using the Ginzburg-Landau (GL) theory. We also discuss their relation to the group velocity and geometric terms. Up to the second-order of the gap function $\Delta_{\mathbf{k}}$, the anapole moment is given by,

$$T_{\mu}^{\text{GL}} = \frac{1}{\beta} \sum_{\mathbf{k}\omega_n} \text{tr} \left[\mathcal{G}_{\mathbf{k}\omega_n}^{\text{p}} \partial_{\mu} H_{\mathbf{k}} \mathcal{G}_{\mathbf{k}\omega_n}^{\text{p}} \Delta_{\mathbf{k}}^{\text{g}} \mathcal{G}_{\mathbf{k}\omega_n}^{\text{h}} \Delta_{\mathbf{k}}^{\text{u}\dagger} - \mathcal{G}_{\mathbf{k}\omega_n}^{\text{p}} \partial_{\mu} H_{\mathbf{k}} \mathcal{G}_{\mathbf{k}\omega_n}^{\text{p}} \Delta_{\mathbf{k}}^{\text{u}\dagger} \mathcal{G}_{\mathbf{k}\omega_n}^{\text{h}} \Delta_{\mathbf{k}}^{\text{g}} \right] + (g \leftrightarrow u), \quad (10)$$

where tr represents the trace over normal state degrees of freedom. Here, $\mathcal{G}_{\mathbf{k}\omega_n}^{\text{p(h)}}$ = $(i\omega_n \mp H_{\mathbf{k}})^{-1}$ is the Green function for the particle (hole) part. The derivation of the formula (10) is shown in Appendix B. From this formula, we see that \mathcal{P} - and \mathcal{T} -symmetry breaking is needed for the anapole superconductivity (see also Appendix B).

We can rewrite the formula in the Bloch band basis,

$$T_{\mu}^{\text{GL}} = \frac{1}{\beta} \sum_{\mathbf{k}\omega_n} \sum_{nmp} \sum_{\chi_n \chi_m \chi_p} C_{nmp\mathbf{k}\omega_n}^{\text{GL}} \text{tr} [P_{n\chi_n \mathbf{k}} \partial_{\mu} H_{\mathbf{k}} P_{m\chi_m \mathbf{k}} \times \left(\Delta_{\mathbf{k}}^{\text{g}} P_{p\chi_p \mathbf{k}} \Delta_{\mathbf{k}}^{\text{u}\dagger} - \Delta_{\mathbf{k}}^{\text{u}\dagger} P_{p\chi_p \mathbf{k}} \Delta_{\mathbf{k}}^{\text{g}} \right)] + (g \leftrightarrow u), \quad (11)$$

where $C_{nmp\mathbf{k}\omega_n}^{\text{GL}} = (i\omega_n - \epsilon_{n\mathbf{k}})^{-1} (i\omega_n - \epsilon_{m\mathbf{k}})^{-1} (i\omega_n + \epsilon_{p\mathbf{k}})^{-1}$, and $P_{n\chi_n \mathbf{k}} = |u_{n\chi_n \mathbf{k}}\rangle \langle u_{n\chi_n \mathbf{k}}|$ is the projection operator. For $n = m = p$, the summand of Eq. (11) vanishes (see Appendix C for details). Therefore, at least two pairs of n , m and p must be nonequivalent for a finite contribution to the anapole moment. In other words, two interband processes are necessary for the anapole superconductivity.

The above necessary condition for n , m and p can be satisfied in three cases. The first case, $n = m \neq p$, corresponds to the group velocity term, and the odd- and even-parity interband pairings play the role of two interband processes. In the following subsection, it is shown that the group velocity term is closely related to the asymmetric BS. The effect of asymmetric BS on the group velocity term is also discussed in Appendix D.

The remaining two cases correspond to the geometric term since the Berry connection is necessary. In the second case, $n \neq m$ and $n = p$ (or $m = p$), the Berry connection of Bloch electrons and either odd-parity or even-parity interband pairing play the role of two interband processes. Finally, in the third case, $n \neq m \neq p \neq n$, all of the even-parity interband pairing, odd-parity interband pairing, and the Berry connection appear in the contribution to the anapole moment. In both cases, via the Berry connection, the Bloch electrons undergo an interband transition from the initial band to the different band, which is coupled to the initial band through the interband Cooper pairs. Thus, the two or more interband processes, due to the Berry connection and interband Cooper

pairs, induce the anapole moment, which is a physical picture of quantum-geometry-induced anapole superconductivity.

B. General two-band model

Next, for a more transparent understanding, we derive the anapole moment in general two-band superconductors with Kramers degeneracy. Although we here adopt a two-band model, the following results can be applied to any multi-band model with multiple bands near the Fermi surface. The normal-state Hamiltonian is written as,

$$H_{\mathbf{k}} = h_{0\mathbf{k}} \mathbf{1} + \mathbf{h}_{\mathbf{k}} \cdot \boldsymbol{\gamma}, \quad (12)$$

by using the 4×4 gamma matrices $\boldsymbol{\gamma} = (\gamma_1 \cdots \gamma_5)$ that anti-commute each other. Here, $h_{0\mathbf{k}}$ and $\mathbf{h}_{\mathbf{k}} = (h_{1\mathbf{k}} \cdots h_{5\mathbf{k}})$ depend on the details of the model. The energy dispersion is given by $\epsilon_{\pm, \mathbf{k}} = h_{0\mathbf{k}} \pm |\mathbf{h}_{\mathbf{k}}|$. Note that the 4 by 4 normal-state Hamiltonian has two bands due to the Kramers degeneracy.

The \mathcal{PT} -symmetric parity-mixed pair potential is expressed as²⁸,

$$\Delta_{\mathbf{k}} = \Delta_{\mathbf{k}}^{\text{g}} + \Delta_{\mathbf{k}}^{\text{u}}, \quad (13)$$

$$\Delta_{\mathbf{k}}^{\text{g}} = \eta_{0\mathbf{k}} \mathbf{1} + \boldsymbol{\eta}_{\mathbf{k}} \cdot \boldsymbol{\gamma}, \quad \Delta_{\mathbf{k}}^{\text{u}} = \frac{i}{2} \sum_{ij} \tilde{\eta}_{ij\mathbf{k}} \gamma_i \gamma_j, \quad (14)$$

where $\eta_{0\mathbf{k}}$, $\boldsymbol{\eta}_{\mathbf{k}} = (\eta_{1\mathbf{k}} \cdots \eta_{5\mathbf{k}})$ and $\tilde{\eta}_{ij\mathbf{k}} = -\tilde{\eta}_{ji\mathbf{k}}$ are the complex valued order parameters for even- and odd-parity pairing channels. Here, taking appropriate U(1) gauge, $\eta_{0\mathbf{k}}$ and $\eta_{i\mathbf{k}}$ are real while $\tilde{\eta}_{ij\mathbf{k}}$ becomes pure imaginary.

Because of the Kramers degeneracy, the particle Green function can be projected to the two degenerate bands as⁶³

$$\mathcal{G}_{\mathbf{k}\omega_n}^{\text{p}} = a_{\mathbf{k}\omega_n} \mathbf{1} + b_{\mathbf{k}\omega_n} \tilde{H}_{\mathbf{k}}, \quad (15)$$

$$a_{\mathbf{k}\omega_n} = \frac{1}{2} \sum_{\pm} (i\omega_n - h_{0\mathbf{k}} \pm |\mathbf{h}_{\mathbf{k}}|)^{-1}, \quad (16)$$

$$b_{\mathbf{k}\omega_n} = \frac{1}{2} \sum_{\pm} \mp (i\omega_n - h_{0\mathbf{k}} \pm |\mathbf{h}_{\mathbf{k}}|)^{-1}, \quad (17)$$

with $\tilde{H}_{\mathbf{k}} = (\mathbf{h}_{\mathbf{k}} \cdot \boldsymbol{\gamma}) / |\mathbf{h}_{\mathbf{k}}| = \hat{\mathbf{h}}_{\mathbf{k}} \cdot \boldsymbol{\gamma}$. The hole Green function is also given by,

$$\mathcal{G}_{\mathbf{k}\omega_n}^{\text{h}} = c_{\mathbf{k}\omega_n} \mathbf{1} + d_{\mathbf{k}\omega_n} \tilde{H}_{\mathbf{k}}, \quad (18)$$

where $a_{\mathbf{k}\omega_n} = -c_{\mathbf{k}-\omega_n}$ and $b_{\mathbf{k}\omega_n} = -d_{\mathbf{k}-\omega_n}$. Hereafter, we omit the (\mathbf{k}, ω_n) dependence for simplicity. Inserting these expressions of Green functions into Eq. (10), we get

$$T_{\mu}^{\text{GL}} = \frac{1}{\beta} \sum_{\mathbf{k}} \sum_{\omega_n} \left(a^2 \text{ctr} \left[\partial H M_{-}^{(1)} \right] + a^2 \text{dtr} \left[\partial H M_{-}^{(2)} \right] + ab \text{ctr} \left[\left\{ \partial H, \tilde{H} \right\} M_{-}^{(1)} \right] + ab \text{dtr} \left[\left\{ \partial H, \tilde{H} \right\} M_{-}^{(2)} \right] + b^2 \text{ctr} \left[\tilde{H} \partial H \tilde{H} M_{-}^{(1)} \right] + b^2 \text{dtr} \left[\tilde{H} \partial H \tilde{H} M_{-}^{(2)} \right] \right). \quad (19)$$

Here, we introduce the \mathcal{P} - and \mathcal{T} -odd bilinear products^{28,33,63,64},

$$M_{-}^{(1)} = \left[\Delta_{\mathbf{k}}^{\text{g}}, \Delta_{\mathbf{k}}^{\text{u}\dagger} \right] + (g \leftrightarrow u), \quad (20)$$

$$M_{-}^{(2)} = \left[\Delta_{\mathbf{k}}^{\text{g}} \tilde{H} \Delta_{\mathbf{k}}^{\text{u}\dagger} - \Delta_{\mathbf{k}}^{\text{u}\dagger} \tilde{H} \Delta_{\mathbf{k}}^{\text{g}} \right] + (g \leftrightarrow u). \quad (21)$$

According to Eq. (19), the presence of finite bilinear products is a necessary condition for the anapole superconductivity.

One of the bilinear products $M_-^{(1)}$ is obtained as,

$$M_-^{(1)} = \mathbf{m}_1 \cdot \boldsymbol{\gamma}, \quad (22)$$

$$[\mathbf{m}_1]_j = -4 \sum_{i(\neq j)} \text{Im} [\eta_i \tilde{\eta}_{ij}^*]. \quad (23)$$

It has been shown that $M_-^{(1)}$ is needed for the asymmetric BS²⁸, and thus, \mathbf{m}_1 represents the role of the asymmetric BS. More specifically, the necessary condition of the asymmetric BS is given by $\mathbf{m}_1 \cdot \hat{\mathbf{h}} \neq 0$ ²⁸. To elucidate the origin and physical meaning of another bilinear product $M_-^{(2)}$, we introduce the interband and intraband superconducting fitness (SCF)^{65,66}, $F_{g(u)}^C$ and $F_{g(u)}^A$, which are defined by

$$F_{g(u)}^C = [\tilde{H}, \boldsymbol{\Delta}^{g(u)}], \quad F_{g(u)}^A = \{\tilde{H}, \boldsymbol{\Delta}^{g(u)}\}. \quad (24)$$

Using this, we can rewrite $M_-^{(2)}$ as,

$$M_-^{(2)} = \frac{1}{4} ([F_g^A, \boldsymbol{\Delta}^{u\dagger}] + [F_u^A, \boldsymbol{\Delta}^{g\dagger}] - \{F_g^C, \boldsymbol{\Delta}^{u\dagger}\} - \{F_u^C, \boldsymbol{\Delta}^{g\dagger}\}) + \text{h.c.} \quad (25)$$

This means that both interband and intraband pairings lead to a finite bilinear product $M_-^{(2)}$. Each term in Eq. (25) is calculated as,

$$[F_g^A, \boldsymbol{\Delta}^{u\dagger}] + \text{h.c.} = 2\mathbf{m}_2 \cdot \boldsymbol{\gamma}, \quad (26)$$

$$[F_u^A, \boldsymbol{\Delta}^{g\dagger}] + \text{h.c.} = 2\mathbf{m}_3 \cdot \boldsymbol{\gamma}, \quad (27)$$

$$\{F_g^C, \boldsymbol{\Delta}^{u\dagger}\} + \text{h.c.} = -2\mathbf{m}_3 \cdot \boldsymbol{\gamma} + 2(\mathbf{m}_1 \cdot \hat{\mathbf{h}})\mathbf{1}, \quad (28)$$

$$\{F_u^C, \boldsymbol{\Delta}^{g\dagger}\} + \text{h.c.} = -2\mathbf{m}_2 \cdot \boldsymbol{\gamma} + 2(\mathbf{m}_1 \cdot \hat{\mathbf{h}})\mathbf{1}, \quad (29)$$

where,

$$[\mathbf{m}_2]_j = -4 \sum_{i(\neq j)} \hat{h}_i \text{Im} [\eta_0 \tilde{\eta}_{ij}^*], \quad (30)$$

$$[\mathbf{m}_3]_j = -2 \sum_{i_1 i_2 i_3 i_4} \varepsilon_{i_1 i_2 i_3 i_4} \hat{h}_{i_1} \text{Im} [\eta_{i_2} \tilde{\eta}_{i_3 i_4}^*]. \quad (31)$$

Here, we use the relationship,

$$\gamma_j = \frac{-1}{4!} \sum_{i_1 i_2 i_3 i_4} \varepsilon_{j i_1 i_2 i_3 i_4} \gamma_{i_1} \gamma_{i_2} \gamma_{i_3} \gamma_{i_4}, \quad (32)$$

with the Levi-Civita tensor $\varepsilon_{i_1 i_2 i_3 i_4 i_5}$. Inserting these expressions into Eq. (25), we obtain,

$$M_-^{(2)} = -(\mathbf{m}_1 \cdot \hat{\mathbf{h}})\mathbf{1} + (\mathbf{m}_2 + \mathbf{m}_3) \cdot \boldsymbol{\gamma}. \quad (33)$$

The first term comes from the asymmetric BS, which originates from the interband SCF. On the other hand, the second and third terms arise from either the intraband SCF and interband SCF. To be more precise, the term $\mathbf{m}_2 \cdot \boldsymbol{\gamma}$ ($\mathbf{m}_3 \cdot \boldsymbol{\gamma}$) needs the \mathcal{P} -even (\mathcal{P} -odd) intraband SCF or the \mathcal{P} -odd (\mathcal{P} -even) interband SCF. This implies that \mathbf{m}_2 (\mathbf{m}_3) contains information of even-parity (odd-parity) intraband pairing and odd-parity

(even-parity) interband pairing. Thus, introducing the SCF helps understand the role of \mathcal{P} -even and \mathcal{P} -odd interband pairings in the anapole superconductivity.

After a tedious but straightforward calculation we can get the group velocity term and geometric term in the GL theory,

$$T^{\text{GL}} = T^{\text{GL:velo}} + T^{\text{GL:geom}}, \quad (34)$$

$$T^{\text{GL:velo}} = \frac{4}{\beta} \sum_{\mathbf{k}\omega_n} [(2abc - a^2d - b^2d) \partial h_0 - (2abd - a^2c - b^2c) \partial |\mathbf{h}|] \mathbf{m}_1 \cdot \hat{\mathbf{h}}, \quad (35)$$

$$T^{\text{GL:geom}} = \frac{4}{\beta} \sum_{\mathbf{k}\omega_n} (a^2 - b^2) |\mathbf{h}| \partial \hat{\mathbf{h}} \cdot [c\mathbf{m}_1 + d(\mathbf{m}_2 + \mathbf{m}_3)]. \quad (36)$$

It should be noticed that the group velocity term contains a factor $\mathbf{m}_1 \cdot \hat{\mathbf{h}}$, which is closely related to the asymmetric BS. Therefore, we conclude that the asymmetric BS is an origin of the group velocity term (see also Appendix D for a simple case).

On the other hand, the Berry connection is essential for the geometric term, as Eq. (36) contains $\partial \hat{\mathbf{h}}$ which makes the Berry connection finite. More specifically, the geometric term arises from various contributions, which are understood by Eq. (36). For the first term of Eq. (36), in addition to the Berry connection, asymmetric BS is also essential in this contribution. In contrast, the second (third) term of Eq. (11) can be finite without even- (odd)-parity interband pairing. Thus, either odd-parity or even-parity interband pairing causes the anapole superconductivity owing to the quantum geometry, although the group velocity term needs both odd-parity and even-parity interband pairing. In other words, whenever the group velocity term is finite, finite Berry connection ensures the presence of the geometric term. Moreover, even when the group velocity term is absent, the geometric term can be finite due to \mathbf{m}_2 and \mathbf{m}_1 . Therefore, necessary conditions for the anapole superconductivity are relaxed by appropriately considering the quantum geometric effect, which was neglected in Ref. 28. Later, we will also show that the anapole moment is dominated by the geometric term at low temperatures.

IV. QUANTUM-GEOMETRY-INDUCED ANAPOLE SUPERCONDUCTIVITY IN UTe₂

In this section, we first show a general theory for anapole superconductivity in locally noncentrosymmetric superconductors (Sec. IV A) and next focus on UTe₂ (Secs. IV B and IV C).

A. Locally noncentrosymmetric superconductors

Many exotic superconductors of recent interest have multiple sublattices which do not lie on the inversion center. UTe₂¹³ and CeRh₂As₂⁶⁷ are examples of such locally noncentrosymmetric superconductors, and a part of materials is listed in a review article⁶⁸. Before demonstrating the quantum-geometry-

TABLE I. Correspondence between Pauli and Dirac matrices.

Pauli	Dirac
$\sigma \otimes \tau_z$	$(\gamma_1 \ \gamma_2 \ \gamma_3)$
$\sigma \otimes \tau_y$	$(-i\gamma_1\gamma_4 \ -i\gamma_2\gamma_4 \ -i\gamma_3\gamma_4)$
$\sigma \otimes \tau_x$	$(i\gamma_1\gamma_5 \ i\gamma_2\gamma_5 \ i\gamma_3\gamma_5)$
$\sigma \otimes \tau_0$	$(-i\gamma_2\gamma_3 \ i\gamma_1\gamma_3 \ -i\gamma_1\gamma_2)$
$\sigma_0 \otimes \tau$	$(\gamma_4 \ \gamma_5 \ -i\gamma_4\gamma_5)$

induced anapole superconductivity in UTe₂, we show that the locally noncentrosymmetric superconductors are generically the platform of anapole superconductivity and clarify the conditions for it. While the following discussions in this subsection are based on the GL expansion, the BCS theory reproduces the results for the anapole moment quantitatively, as shown in Sec. IV C.

We consider the locally noncentrosymmetric two-sublattice model²⁸, which is adopted as a minimal model for UTe₂ later,

$$H = \xi\sigma_0 \otimes \tau_0 + w_x\sigma_0 \otimes \tau_x + w_y\sigma_0 \otimes \tau_y + \mathbf{g} \cdot \boldsymbol{\sigma} \otimes \tau_z, \quad (37)$$

$$\Delta^g = \Delta^g \left[\sum_{\mu=0,x,y} \phi_g^\mu \sigma_0 \otimes \tau_\mu + \mathbf{d}_g^z \cdot \boldsymbol{\sigma} \otimes \tau_z \right], \quad (38)$$

$$\Delta^u = \Delta^u \left[\sum_{\mu=0,x,y} \mathbf{d}_u^\mu \cdot \boldsymbol{\sigma} \otimes \tau_\mu + \phi_u^z \sigma_0 \otimes \tau_z \right]. \quad (39)$$

Here, σ_μ and τ_μ are the Pauli matrices for the spin and sublattice spaces, ξ is the single-particle kinetic energy, and $\mathbf{g} = (g_x, g_y, g_z)$ is the staggered-type ASOC due to the local \mathcal{P} -symmetry breaking at atomic sites. For example, in UTe₂, U atoms form a ladder structure, which consists of two sublattices lacking the \mathcal{P} -symmetry at the atomic sites. The local point group descends to C_{2v} from D_{2h} , and therefore, the Rashba ASOC naturally appears. Since the two sublattices are related by the global \mathcal{P} -symmetry, the Rashba ASOC shows a staggered form proportional to τ_z .

The superconducting pair potentials are divided into the spin-singlet component $\phi_{g(u)}^\mu$ and the spin-triplet component $\mathbf{d}_{g(u)}^\mu$. The local inversion symmetry breaking also leads to sublattice-dependent parity-mixing of the pair potential. Thus, the sublattice-independent spin-singlet (spin-triplet) pairing component and the staggered spin-triplet (spin-singlet) one coexist in the even-parity (odd-parity) pair potential. To preserve the \mathcal{PT} -symmetry while breaking the \mathcal{T} -symmetry, the relative phase between the complex-valued order parameters Δ^g and Δ^u is assumed to be $\pi/2$, and thus, $4\text{Im}(\Delta^g\Delta^{u*}) \neq 0$.

We show the correspondence between the Pauli matrices and the Dirac matrices in Table I⁶⁹, from which the condition for anapole superconductivity can be derived based on the discussions in Sec. III. The results are summarized in Table II, where conditions for the finite group velocity term and the geometric term are explicitly presented. Here, we define $\hat{\mathbf{g}} = \mathbf{g}/|\mathbf{h}|$ and $\hat{w}_{x(y)} = w_{x(y)}/|\mathbf{h}|$ with $|\mathbf{h}| = \sqrt{w_x^2 + w_y^2 + |\mathbf{g}|^2}$.

Note that all the terms of anapole moment is proportional to $4\text{Im}(\Delta^g\Delta^{u*})$, which is finite by assumption. The geometric term can be finite in a relatively simple situation. For example, the m_2 -term gives a finite anapole moment when $\phi_g^0(\hat{\mathbf{g}} \times \mathbf{d}_u^0) \cdot \partial\hat{\mathbf{g}} \neq 0$. This condition is satisfied in the presence of an usual spin-singlet pairing component ϕ_g^0 and an interband pairing component $\hat{\mathbf{g}} \times \mathbf{d}_u^0$ when the corresponding Berry connection is finite. If the $s + ip$ -wave pairing state is realized in UTe₂ as proposed¹⁴, the even-parity s -wave component, ϕ_g^0 , and the odd-parity p -wave component, \mathbf{d}_u^0 , naturally exist, and the Berry connection arises from the staggered Rashba ASOC. Thus, the anapole superconductivity is likely to occur in UTe₂ owing to the quantum geometry when the $s + ip$ -wave state is stabilized.

TABLE II. Conditions for the anapole superconductivity in locally noncentrosymmetric systems. The corresponding SCF is also shown. We assume $4\text{Im}(\Delta^g\Delta^{u*}) \neq 0$, which is satisfied in the parity-mixed \mathcal{T} -symmetry breaking superconductors. When an inequality listed in the table is satisfied, (a) the group velocity term and (b) the geometric term are finite.

(a) Group velocity term		
Condition (Dirac)	Condition (Pauli)	SCF
	$\partial\epsilon_\pm \mathbf{d}_g^z \cdot \mathbf{d}_u^{y(x)} \hat{w}_{x(y)} \neq 0$	
$\partial\epsilon_\pm m_1 \cdot \hat{\mathbf{h}} \neq 0$	$\partial\epsilon_\pm \phi_g^{y(x)} \phi_u^z \hat{w}_{x(y)} \neq 0$ $\partial\epsilon_\pm \phi_g^{y(x)} \mathbf{d}_u^{x(y)} \cdot \hat{\mathbf{g}} \neq 0$ $\partial\epsilon_\pm (\mathbf{d}_g^z \times \mathbf{d}_u^0) \cdot \hat{\mathbf{g}} \neq 0$	$F_g^C, F_u^C \neq 0$
(b) Geometric term		
Condition (Dirac)	Condition (Pauli)	SCF
	$\mathbf{d}_g^z \cdot \mathbf{d}_u^{y(x)} \partial\hat{w}_{x(y)} \neq 0$	
$m_1 \cdot \partial\hat{\mathbf{h}} \neq 0$	$\phi_g^{y(x)} \phi_u^z \partial\hat{w}_{x(y)} \neq 0$ $\phi_g^{y(x)} \mathbf{d}_u^{x(y)} \cdot \partial\hat{\mathbf{g}} \neq 0$ $(\mathbf{d}_g^z \times \mathbf{d}_u^0) \cdot \partial\hat{\mathbf{g}} \neq 0$	$F_g^C, F_u^C \neq 0$
	$\phi_g^0 \hat{\mathbf{g}} \cdot \mathbf{d}_u^{y(x)} \partial\hat{w}_{x(y)} \neq 0$	
$m_2 \cdot \partial\hat{\mathbf{h}} \neq 0$	$\phi_g^0 \hat{w}_{y(x)} \phi_u^z \partial\hat{w}_{x(y)} \neq 0$ $\phi_g^0 \hat{w}_{y(x)} \mathbf{d}_u^{x(y)} \cdot \partial\hat{\mathbf{g}} \neq 0$ $\phi_g^0 (\hat{\mathbf{g}} \times \mathbf{d}_u^0) \cdot \partial\hat{\mathbf{g}} \neq 0$	$F_g^A, F_u^C \neq 0$
	$\hat{\mathbf{g}} \cdot (\mathbf{d}_g^z \times \mathbf{d}_u^{y(x)}) \partial\hat{w}_{y(x)} \neq 0$	
	$\hat{w}_{x(y)} \mathbf{d}_g^z \cdot \mathbf{d}_u^0 \partial\hat{w}_{y(x)} \neq 0$	
	$\hat{\mathbf{g}} \cdot (\phi_g^{x(y)} \mathbf{d}_u^0) \partial\hat{w}_{y(x)} \neq 0$	
$m_3 \cdot \partial\hat{\mathbf{h}} \neq 0$	$\hat{w}_{x(y)} (\mathbf{d}_g^z \times \mathbf{d}_u^{x(y)}) \cdot \partial\hat{\mathbf{g}} \neq 0$ $\hat{w}_{x(y)} \phi_g^{y(x)} \mathbf{d}_u^0 \cdot \partial\hat{\mathbf{g}} \neq 0$ $(\hat{\mathbf{g}} \times (\phi_g^{x(y)} \mathbf{d}_u^{x(y)})) \cdot \partial\hat{\mathbf{g}} \neq 0$ $(\hat{\mathbf{g}} \times \mathbf{d}_g^z \phi_u^z) \cdot \partial\hat{\mathbf{g}} \neq 0$	$F_g^C, F_u^A \neq 0$

B. Symmetry classification in the D_{2h} point group

Here, we show the classification of parity-mixed superconducting states assuming the crystals of D_{2h} point group symmetry with UTe₂ in mind. Combination of the four even-

parity irreducible representations ($A_g, B_{1g}, B_{2g}, B_{3g}$) and odd-parity ones ($A_u, B_{1u}, B_{2u}, B_{3u}$) gives $4 \times 4 = 16$ classes of parity-mixed pairing states. They are classified into either the anapole superconductivity or monopole superconductivity.

The anapole superconducting state has the polarity and shares the symmetry with the magnetic toroidal ordered state, while the monopole superconducting state is an superconducting analog of the magnetic monopole state⁷⁰. In the D_{2h} point group, the order parameter of anapole superconductivity breaks the C_2 rotation symmetry which flips the polar axis. In contrast, the C_2 rotation symmetry of all directions are preserved in the monopole superconducting state, which means that the anapole moment vanishes and the finite- q pairing states are prohibited.

TABLE III. Classification of parity-mixed superconducting states in the D_{2h} point group symmetry. Direction of anapole moment is shown for the anapole superconducting state. The other pairing states are monopole superconducting states and represented as "monopole".

	A_g	B_{1g}	B_{2g}	B_{3g}
A_u	monopole	T_z	T_y	T_x
B_{1u}	T_z	monopole	T_x	T_y
B_{2u}	T_y	T_x	monopole	T_z
B_{3u}	T_x	T_y	T_z	monopole

Table III shows the finite component of the anapole moment for the 12 anapole superconducting states, while we denote "monopole" for the monopole superconducting state. For instance, $A_g + iB_{3u}$ pairing state is a anapole superconducting state with anapole moment along the x -axis. On the other hand, $A_g + iA_u$ pairing state is a non-polar monopole superconducting state, where the anapole moment vanishes.

C. Anapole superconductivity in UTe_2

In the theoretical calculation which constructs a 24-orbital model for UTe_2 ¹⁴, competing ferromagnetic and antiferromagnetic fluctuations have been shown, implying the competition between the s -wave and p -wave pairings. Comparing the theoretical results with the experimentally observed multiple superconducting phases, the parity-mixed \mathcal{T} -symmetry-broken $s + ip$ -wave state was proposed for UTe_2 . Such $s + ip$ -wave superconducting state was also discussed in experimental studies^{71,72}. In this scenario, \mathcal{P} - and \mathcal{T} -symmetry breaking necessary for the anapole superconductivity is predicted. To examine the possible anapole superconductivity in UTe_2 , we adopt a model for UTe_2 and show unique features which have microscopic origins beyond the GL theory.

Here, one of the purposes is to derive the minimal condition and universal properties of anapole superconductivity, which are independent of the detailed band structure. Therefore, we focus on the sublattice and spin degrees of freedom in UTe_2 , giving rise to multiple bands near the Fermi level. Actually, most of the following results are independent of the details of band structure, as is also discussed in Sec. V. Thus, we set the

normal-state Hamiltonian Eq. (37) as

$$w_x = w_y = 0, \quad (40)$$

$$\xi = t \sum_{\mu} \cos k_{\mu} - \mu, \quad (41)$$

$$\mathbf{g} = \alpha (\sin k_y, -\sin k_x, 0), \quad (42)$$

with $(t, \mu, \alpha) = (0.2, 0.4, \pm 0.04)$. In this model, the energy dispersion is given by $\epsilon_{\pm} = \xi \pm |\mathbf{g}|$. In Table II, some terms of the anapole moment are first order in \mathbf{g} , implying that the anapole moment may depend on the sign of the ASOC coupling constant α . Thus, we examine the two cases, $\alpha = \pm 0.04$. We will actually show that the properties of anapole superconductivity depend on the sign of α .

First, we consider the superconducting pair potential,

$$\Delta^g(T) = \Delta_0(T) \phi_g^0 \sigma_0 \otimes \tau_0, \quad (43)$$

$$\Delta^u(T) = i \Delta_0(T) d_{u,z}^0 \sigma_z \otimes \tau_0, \quad (44)$$

with $\phi_g^0 = 1$ and $d_{u,z}^0 = \sin k_y$, which belongs to the $A_g + iB_{3u}$ irreducible representation of D_{2h} point group. The temperature dependence is assumed to be $\Delta_0(T) = \Delta_0^{\max} \tanh(1.74 \sqrt{(T_c - T)/T})$, where $\Delta_0^{\max} = \frac{3.53}{2} T_c = 0.02$.

Based on the GL theory, we expect that the group velocity term vanishes in this case, i.e. $\mathbf{m}_1 \cdot \hat{\mathbf{h}} = 0$. However, since the \mathbf{d} vector for the B_{3u} representation is not parallel to the \mathbf{g} vector for the ASOC of C_{2v} point group, odd-parity interband pairing is always finite in addition to intraband pairing. In other words, $\hat{\mathbf{g}} \times \mathbf{d}_u^0 \neq 0$ leads to odd-parity interband pairing. Therefore, the geometric term is finite because the condition $\mathbf{m}_2 \cdot \partial \hat{\mathbf{h}} = \phi_g^0 (\hat{\mathbf{g}} \times \mathbf{d}_u^0) \cdot \partial \hat{\mathbf{g}} \neq 0$ in Table II(b) is satisfied. As a result, $A_g + iB_{3u}$ representation of superconductivity in UTe_2 ensures the presence of the quantum-geometry-induced anapole superconductivity regardless of the size of the interband pairing.

We calculate the anapole moment by Eqs. (6)-(8) and show the temperature dependence of T_x in Fig. 1(a). Note that $T_y = T_z = 0$ owing to the symmetry of $A_g + iB_{3u}$ irreducible representation (Table III). The anapole moment does not depend on the sign of α in this case. We denote the total anapole moment as T_{μ}^a in all figures to avoid the confusion with the temperature T . We find that the group velocity term (orange line) is always zero, revealing that the prediction based on the GL theory is exact. Therefore, the geometric term (blue line) determines the anapole moment (pink line). In Fig. 1(b), we also plot the superfluid weight D_{xx}^s , defined as the second-order q -derivative of the free energy at $q = 0$ (see Appendix E for details). We can evaluate the center of mass momentum of Cooper pairs in the anapole superconducting state by $-T_x/D_{xx}^s$ (see Appendix E). We also directly calculate the center of mass momentum q_c , which minimizes the free energy, and compare it with $-T_x/D_{xx}^s$ in Fig. 1(b). Since $-T_x/D_{xx}^s$ almost coincides with q_c , we confirm that $-T_x/D_{xx}^s$ provides a good estimation for q_c , indicating that higher-order q -derivatives can be ignored. Thus, we conclude that the finite- q pairing state due to the anapole superconductivity is determined by the anapole moment. We stress that the asymmetric BS does not appear in this model, and

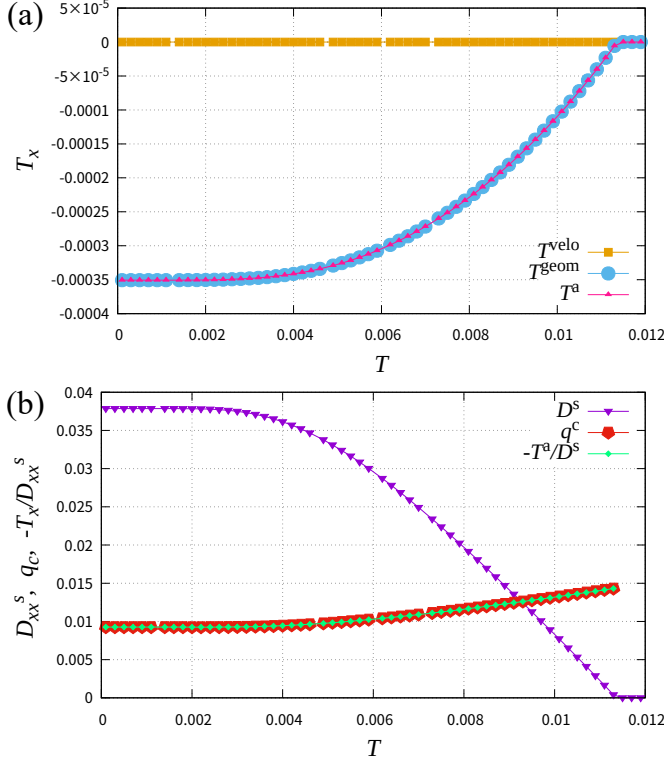


FIG. 1. The temperature dependence of the anapole moment for the pair potential Eqs. (43) and (44). (a) The orange, blue, and pink lines show the group velocity term, geometric term, and total anapole moment, i.e. T_x^{velo} , T_x^{geom} , and T_x , respectively. The blue and pink lines coincide because $T_x^{\text{geom}} = T_x$ in this case. (b) The purple and red lines show the superfluid weight D_{xx}^s and the most stable center of mass momenta of Cooper pairs q_c . We also show $-T_x/D_{xx}^s$ by the green line, which almost coincides with the red line for q_c .

the anapole superconductivity has a purely quantum geometric origin. More specifically, the Berry connection of Bloch electrons and the interband pairing play essential roles.

Next, we consider the superconducting pair potential,

$$\Delta^g(T) = \Delta_0(T) (\phi_g^0 \sigma_0 \otimes \tau_0 + d_{g,y}^z \sigma_y \otimes \tau_z), \quad (45)$$

$$\Delta^u(T) = i\Delta_0(T) d_{u,z}^0 \sigma_z \otimes \tau_0, \quad (46)$$

with $d_{g,y}^z = \sin k_x$, which also belongs to the $A_g + iB_{3u}$ irreducible representation. Thus, $T_y = T_z = 0$ is satisfied as in the previous case. We assume the same temperature dependence of $\Delta_0(T)$ as before. In this case, the group velocity term becomes finite as expected based on the GL theory since the condition, $\partial(h_0 \pm |h|) \mathbf{m}_1 \cdot \hat{\mathbf{h}} = \partial\epsilon_{\pm} (d_g^z \times d_u^0) \cdot \hat{\mathbf{g}} \neq 0$, in Table II(a) is satisfied. Similarly, the geometric term is also finite because $\mathbf{m}_1 \cdot \partial\hat{\mathbf{h}} = (d_g^z \times d_u^0) \cdot \partial\hat{\mathbf{g}}$ and $\mathbf{m}_2 \cdot \partial\hat{\mathbf{h}} = \phi_g^0 (\hat{\mathbf{g}} \times d_u^0) \cdot \partial\hat{\mathbf{g}}$ are finite. As the group velocity term is first order in α according to the GL theory, we expect that the sign of the ASOC coupling constant α is essential for the group velocity term⁷³. In addition, a part of the geometric term due to $\mathbf{m}_1 \cdot \partial\hat{\mathbf{h}}$ is the first-order term, and the sign of α also affects the geometric term.

In Figs. 2(a) and 2(b), we show the temperature dependence of the anapole moment for $\alpha = 0.04$ and $\alpha = -0.04$, respectively. We also show the superfluid weight and q_c in Figs. 2(c) and 2(d). We find that the sign of α drastically changes the group velocity term, whose sign is opposite between $\alpha = 0.04$ and $\alpha = -0.04$. The magnitude is different between the two cases, provably due to an effect beyond the GL theory. On the other hand, the sign of the Rashba ASOC α only slightly changes the geometric term. Note that other physical quantities also depend on the sign of α since the band representation of the gap function depends on α , as $\phi_g^0 + d_{g,y}^z g_y / |g|$. Actually, we see that the superfluid weight depends on the sign of α .

In both Figs. 2(a) and 2(b), the group velocity term decays in the low temperature regime, which is attributed to the fact that the group velocity term is induced by the asymmetric BS. The asymmetric BS, namely, $E_{ak} \neq E_{a-k}$, leads to non-equivalent distribution of Bogoliubov quasiparticles, $f(E_{ak}) \neq f(E_{a-k})$. This effect mainly induces the group velocity term. However, the Fermi distribution function is reduced to the step function in the low temperature region, $f(E_{ak}) \simeq \theta(-E_{ak})$, which leads to $f(E_{ak}) \simeq f(E_{a-k})$ in the gapped system and suppresses the group velocity term (see also Appendix D). Therefore, the anapole moment is mainly determined by the geometric term in the low temperature region. On the other hand, the relation $\theta(E_{ak}) = \theta(E_{a-k})$ does not hold when the BFS are present. Thus, the group velocity term can be sizable at $T = 0$ when large BFS appear at $q = 0$. This case is shown in Appendix D.

In the model adopted in this section, while the BFS do not exist at $q = 0$, they appear in the anapole superconducting state as a result of the center of mass momentum of Cooper pairs. In Figs. 3(a) and 3(b), we show the BS in the stable state $q = q_c \hat{x}$ for $\alpha = 0.04$ and $\alpha = -0.04$, respectively. In the figures, the inset shows the presence of BFS. In our model for $q = 0$, the spin-triplet pairing component of the pair potential gives rise to the anisotropic gap structure. Therefore, Bogoliubov quasiparticles with almost zero energy are present. As a result, when the anapole moment tilts the BS along the direction of $q = q_c \hat{x}$, the BFS appear near the gap minimum. Therefore, the anapole superconductivity can be verified by measuring the BFS.

Finally, we show an intriguing phenomenon originating from the competition of the group velocity and geometric terms in the anapole moment. In Figs. 2(a) and 2(c), the anapole moment as well as q_c change the sign as the temperature decreases. This is because the geometric term has the opposite sign of the group velocity term and the group velocity term vanishes at the zero temperature. As we mentioned above, the BFS are absent when the anapole moment is small $T_x \simeq 0$, while they appear for large T_x . Therefore, the BFS appear below $T = T_c$, disappear in the intermediate temperature region, and reappear in the low temperature region by following the non-monotonic temperature dependence of the anapole moment. This is confirmed by the temperature dependence of DOS in Fig. 4. The DOS at the Fermi level is zero around $T = 0.0085$ since the anapole moment is small. On the other hand, the DOS is finite in the high and low tem-

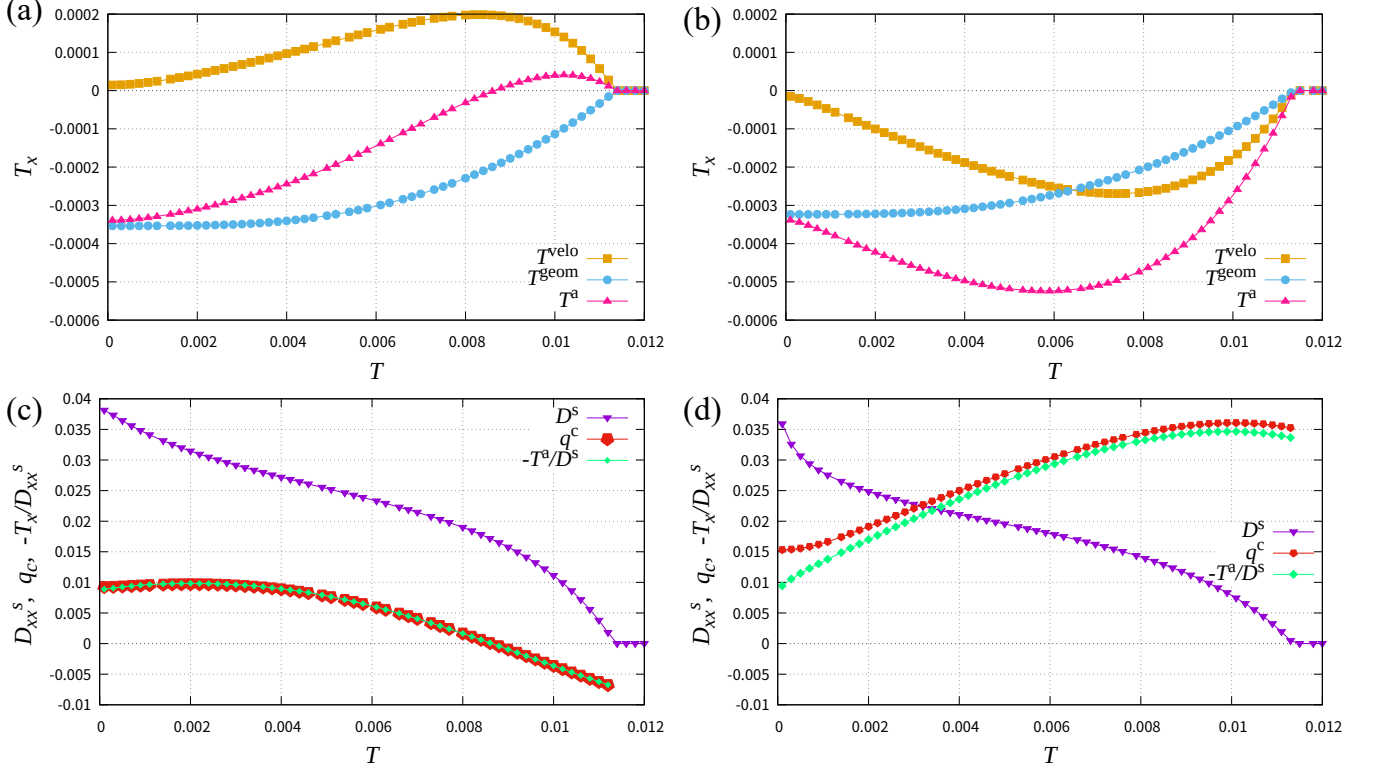


FIG. 2. (a) (b) The anapole moment and (c) (d) the superfluid weight and q_c for the pair potential Eqs. (45) and (46). We assume $\alpha = 0.04$ in the panels (a) and (c), while $\alpha = -0.04$ in (b) and (d). The lines with colors show the same quantities as in Fig. 1

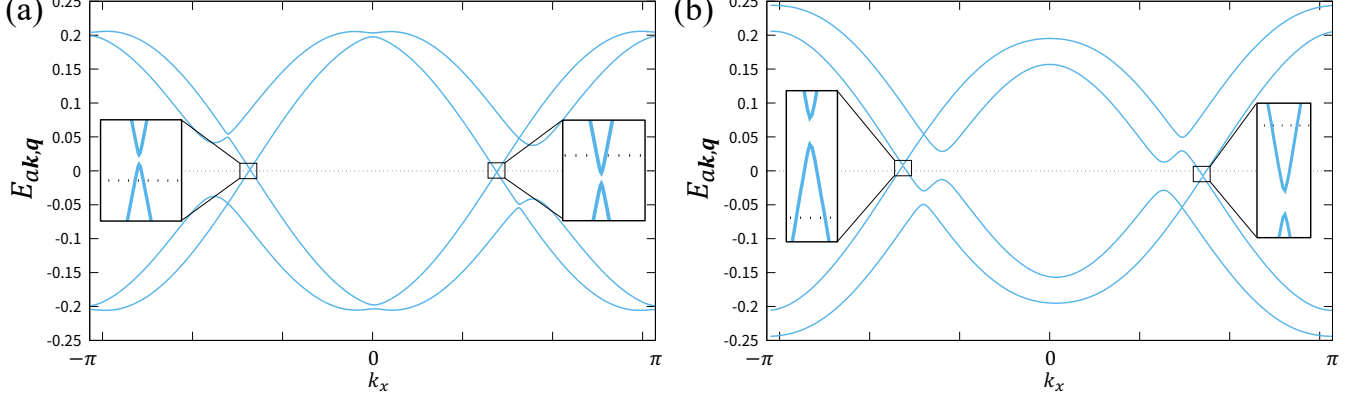


FIG. 3. BS in the anapole superconducting state with $\mathbf{q} = q_c \hat{x}$ for the pair potential Eqs. (45) and (46). Here, we plot $E_{ak,q}$ which follows the eigenvalue equation $H_{k,q}^{\text{BdG}} |\psi_{ak,q}\rangle = E_{ak,q} |\psi_{ak,q}\rangle$. (a) BS on the line $(k_y, k_z) = (-0.0713998, 0)$ for $\alpha = 0.04$ and $T = 0.002$. (b) BS on the line $(k_y, k_z) = (0.499799, 0)$ for $\alpha = -0.04$ and $T = 0.01$. The inset shows the enlarged view, which underlines the presence of BFS.

perature regions where the magnitude of the anapole moment is sizable. This behavior is consistent with the reappearance of BFS, which is a characteristic feature of the anapole superconducting state with competing group velocity and geometric terms. Thus, the role of quantum geometry on anapole superconductivity can be studied by measuring the zero energy DOS.

V. DISCUSSION

In this paper, we showed some unique features of quantum-geometry-induced anapole superconductivity. A candidate material is UTe_2 and our result may pave the way for clarifying the symmetry of superconductivity in UTe_2 . Thus, toward the experimental verification of anapole superconductivity in UTe_2 , we give some discussions in this section.

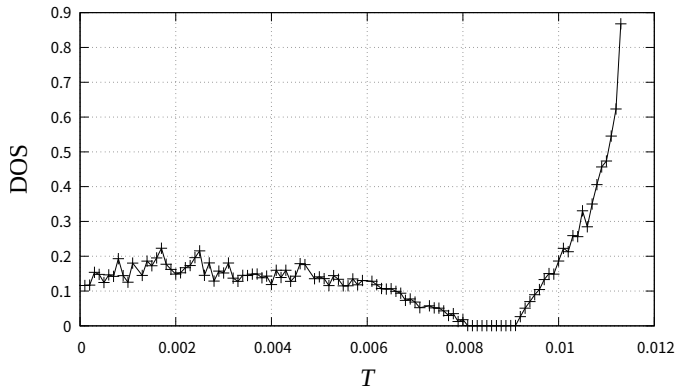


FIG. 4. The temperature dependence of the DOS at the Fermi level calculated by $\sum_{\mathbf{k}} \sum_a \delta / \pi (\delta^2 + E_{a\mathbf{k},q_c}^2)$ with $\delta = 1 \times 10^{-6}$. We assume the same parameters as Figs. 2(a) and 2(c)

A concern which is not limited to UTe_2 is the stability of finite- \mathbf{q} pairing against the quantum fluctuation. For the s -wave superconductivity in the isotropic and continuum model, the mean-field solution of the FFLO superconductivity is known to be unstable due to the quantum fluctuation^{74,75}. This is attributed to the infinite degeneracy of finite- \mathbf{q} pairing states ensured by the isotropic symmetry. In contrast, in the anapole superconductivity, the stable momentum of Cooper pairs \mathbf{q} is restricted to only one direction, and additional degeneracy does not occur. Therefore, it is expected that anapole superconductivity is stable against quantum fluctuation. The argument is also supported by the fact that the finite- \mathbf{q} pairing state is stable in the anisotropic three-dimensional system⁷⁵. Our main target is the anisotropic three-dimensional systems, the case of UTe_2 .

Then, we give some comments and remarks on the results relating to UTe_2 , which include (1) the justification of the results obtained by the simplified model, (2) future issues, (3) methods for observing the anapole superconductivity, and (4) the relationship between our results and the recent experiments.

(1) In this paper, we dealt with a simplified model for UTe_2 , where the orbital degree of freedom, electron correlation effect, detailed band structure, and so on are neglected for simplicity. Therefore, we discuss the situations in which our results are adaptable. First, to derive the quantum-geometry-induced anapole superconductivity in UTe_2 , we only assumed the presence of the ASOC due to the locally noncentrosymmetric structure as characteristic normal state property. Since the presence of the ASOC is universal for the crystal structure of UTe_2 , we conclude that quantum-geometry-induced anapole superconductivity is also realized in more complicated models for UTe_2 . Also, the decay of the group velocity term is universal when the BFS is absent for the zero center of mass momenta of Cooper pairs. Therefore, these results are adaptable for a wide range of the models for UTe_2 .

Next, we comment on the BFS induced by the anapole moment and the sign change of the center of mass momenta, which are model-dependent. For the BFS to appear from the

anapole moment, there must be gap minimum or node which depends on the Fermi surface and the order parameters. Such gap minimum or node is realistic and often obtained in microscopic calculations. Especially, we would like to note that highly anisotropic momentum dependence in both even-parity and odd-parity pair potentials have been obtained based on the periodic Anderson model for UTe_2 ¹⁴. As for the sign change, competition between the geometric and group velocity terms is needed, which also depends on the band structure and order parameters. In addition, in our model the presence or absence of the sign change depends also on the ASOC, which is hard to be predicted. As a result, the sign change of the center of mass momenta and the associated reentrant BFS depends on the model. Thus, the BFS is likely to appear if the anapole superconductivity is realized in UTe_2 , but the reappearing behavior of the BFS is not universal and should be verified by further calculations.

(2) From the above discussion, it is desired to study a more realistic model for UTe_2 , as we have carried out for FeSe based on the first-principles calculation^{58,62}. In a model taking account of various degrees of freedom, we may obtain significant contributions from the quantum geometry. Our previous study⁶² has shown that the band degeneracy near the Fermi surfaces induces a large geometric contribution to the superfluid weight, implying that the band degeneracy may also be advantageous for the quantum-geometry-induced anapole superconductivity.

It is also desired to solve multiple gap equations self-consistently, determining the amplitude and temperature dependence of two-component gap functions. While the necessary condition of the anapole superconductivity does not depend on such details, the self-consistent calculation of realistic models may enable quantitative estimation of the anapole moment, which, in turn, predicts the presence/absence of the sign change of the anapole moment. Such quantitative studies are beyond the scope of this paper and are left for future works.

(3) The anapole superconductivity can also be verified by other methods. For example, the Josephson junction experiment, which was proposed to detect the helical superconductivity^{44,45}, can apply to observe the anapole superconductivity. In addition, a part of the authors proposed a unique vortex structure on anapole domains, current-induced anapole domain switching²⁸, and nonreciprocal optical and Meissner responses^{76,77}. Recently, we also showed the superconducting piezoelectric effect⁴² and intrinsic superconducting diode effect⁷⁸ in the anapole superconductors, which will be presented in another publication⁴³.

(4) We would like to stress that the symmetry of superconductivity in UTe_2 is unsettled. One of unresolved issues is the \mathcal{T} -symmetry breaking in the superconducting state, reported by the STM⁷⁹ and the polar Kerr effect⁸⁰. Here we comment on the unidirectional property observed in the STM. It may be related to the anapole superconductivity, which is a unidirectional superconducting state in the bulk. Further studies are desired and ongoing to elucidate the exotic superconductivity in UTe_2 .

While we focused on the superconducting state at the zero magnetic field in this paper, an anapole superconducting state

with finite- q pairing may also appear at finite magnetic fields. The observation of the double superconducting transitions in UTe_2 under the magnetic field along the b -axis implies the superconducting phases with distinct symmetry^{71,72}. If the superconducting state around $H_b \simeq 15\text{T}$ is the $s + ip$ -wave pairing state as discussed⁷¹, it is either finite- q anapole superconductivity or monopole superconductivity. Although the \mathcal{PT} -symmetry is broken by the magnetic field in this phase, it does not suppress the finite- q pairing. The possibility of anapole superconductivity under the magnetic field is also discussed in Ref. 72.

VI. SUMMARY

In this paper, we showed that the quantum geometry of Bloch electrons induces the anapole superconductivity when the superconducting state breaks the \mathcal{P} - and \mathcal{T} -symmetry and has the polar symmetry. Formulating the anapole moment characterizing the anapole superconductivity thoroughly, we find the group velocity term and geometric term with different origins. Based on the theory a model for UTe_2 was analyzed, and characteristic features of anapole superconductivity were clarified.

We identified microscopic processes for the group velocity term and geometric term of the anapole moment. At least two interband processes are necessary. The previous study²⁸ revealed that the asymmetric BS can induce the anapole superconductivity. This mechanism corresponds to the group velocity term. For the interband processes both even-parity and odd-parity pair potentials must have interband components. In contrast, the normal state Berry connection represents the interband process and gives rise to the geometric term. Since quantum geometry arises from the geometric structure of Bloch wave functions, the geometric term does not need the asymmetric structure of BS. Even when the odd structure of Cooper pairs does not affect the BS, the geometric term can be finite and cause the anapole superconductivity. In other words, the quantum geometry can extract the odd structure of Cooper pairs which does not appear in the BS, and reflect it in the anapole moment. Therefore, the anapole superconductivity may have a quantum geometric origin. This case requires only either even-parity or odd-parity interband pair potential.

Furthermore, we clarified the general and unique features of anapole superconductivity. First, in the low-temperature region, the anapole superconductivity is purely induced by the quantum geometry. This is because the group velocity term is suppressed by the superconducting gap. In other words, the quantum geometry is needed for the anapole superconductivity in the ground state. Second, the BFS appears in the anapole superconducting state, when the gap is sufficiently anisotropic. Third, when the group velocity term and the geometric term are competing, the anapole moment changes the sign as decreasing the temperature. This sign change may lead to the nonmonotonic evolution of the BFS. A candidate superconductor UTe_2 may host an anisotropic superconducting gap¹³, and therefore, the appearance of the BFS is expected.

Observation of the BFS and their unique temperature dependence would not only evidence the anapole superconductivity in UTe_2 but also provide a strong constraint on the symmetry of superconductivity (see Table III for symmetry classification of parity-mixed superconducting states). Therefore, search for BFS in UTe_2 is desirable.

In conclusion, the quantum geometry ubiquitously induces the anapole superconductivity in the \mathcal{PT} -symmetric parity-mixed pairing state in multiband superconductors. The anapole superconducting state may show unique phenomena which can be experimentally tested. Thus, we propose a way to clarify the superconducting state in UTe_2 .

ACKNOWLEDGMENTS

We are grateful to A. Daido, R. Sano, D. Aoki, J.-P. Brison, K. Ishida, Y. Tokiwa, Y. Tokunaga, and D. F. Agterberg for fruitful discussions. This work was supported by JSPS KAKENHI (Grants Nos. JP18H01178, JP18H05227, JP20H05159, JP21K18145, JP22H01181, JP22J22520, JP22H04933), JST SPRING (Grant Number JPMJSP2110) and SPIRITS 2020 of Kyoto University.

Appendix A: Derivation of anapole moment

In this section, we derive the anapole moment in the superconducting state. We start from the BdG Hamiltonian written as,

$$\hat{H}^{\text{BdG}} = \frac{1}{2} \sum_{\mathbf{k}} \hat{\Psi}_{\mathbf{k},q}^\dagger \tilde{H}_{\mathbf{k},q}^{\text{BdG}} \hat{\Psi}_{\mathbf{k},q}, \quad (\text{A1})$$

$$\tilde{H}_{\mathbf{k},q}^{\text{BdG}} = \begin{pmatrix} H_{\mathbf{k}+q} & \Delta_{\mathbf{k}} U_{\mathcal{T}} \\ U_{\mathcal{T}}^\dagger \Delta_{\mathbf{k}}^\dagger & -H_{-\mathbf{k}+q}^T \end{pmatrix}, \quad (\text{A2})$$

$$\hat{\Psi}_{\mathbf{k},q}^\dagger = \begin{pmatrix} \hat{c}_{\mathbf{k}+q}^\dagger & \hat{c}_{-\mathbf{k}+q}^T \end{pmatrix}. \quad (\text{A3})$$

Using the unitary operator,

$$U_{\mathcal{T}_{\text{hole}}} = \begin{pmatrix} \sigma_0 \otimes \mathbf{1} & 0 \\ 0 & U_{\mathcal{T}} \end{pmatrix}, \quad (\text{A4})$$

we can rewrite the BdG Hamiltonian as,

$$\begin{aligned} \hat{H}^{\text{BdG}} &= \frac{1}{2} \sum_{\mathbf{k}} \hat{\Psi}_{\mathbf{k},q}^\dagger U_{\mathcal{T}_{\text{hole}}}^\dagger U_{\mathcal{T}_{\text{hole}}} \tilde{H}_{\mathbf{k},q}^{\text{BdG}} U_{\mathcal{T}_{\text{hole}}}^\dagger U_{\mathcal{T}_{\text{hole}}} \hat{\Psi}_{\mathbf{k},q}, \\ &= \frac{1}{2} \sum_{\mathbf{k}} \hat{\Psi}_{\mathbf{k},q}^\dagger H_{\mathbf{k},q}^{\text{BdG}} \hat{\Psi}_{\mathbf{k},q}. \end{aligned} \quad (\text{A5})$$

Thus, we define the Nambu Green function with Matsubara frequency ω_n as, $\mathcal{G}_{\mathbf{k},q,\omega_n}^{\text{BdG}} = [i\omega_n - H_{\mathbf{k},q}^{\text{BdG}}]^{-1}$. Using this, the free energy is obtained as $F_q = -\frac{1}{2\beta} \sum_{\mathbf{k}\omega_n} \text{Tr} \ln[\mathcal{G}_{\mathbf{k},q,\omega_n}^{\text{BdG}-1}]$, where Tr represents the trace over all internal degrees of freedom. The anapole moment

is defined as the first-order coefficient of the superconducting free energy with respect to \mathbf{q} ²⁸:

$$\begin{aligned}
T_\mu &= \lim_{\mathbf{q} \rightarrow 0} \frac{dF_{\mathbf{q}}}{dq_\mu}, \\
&= \lim_{\mathbf{q} \rightarrow 0} \left(\partial_{q_\mu} F_{\mathbf{q}} + \sum_l \partial_{q_\mu} \Delta_l(\mathbf{q}) \partial_{\Delta_l(\mathbf{q})} F(\mathbf{q}) \right), \\
&= \lim_{\mathbf{q} \rightarrow 0} \partial_{q_\mu} F_{\mathbf{q}}, \\
&= \frac{1}{2\beta} \lim_{\mathbf{q} \rightarrow 0} \sum_{\mathbf{k}\omega_n} \text{Tr} [\mathcal{G}_{\mathbf{k},\mathbf{q},\omega_n}^{\text{BdG}} \partial_{q_\mu} H_{\mathbf{k},\mathbf{q}}^{\text{BdG}}], \\
&= \frac{1}{2\beta} \sum_{\mathbf{k}\omega_n} \text{Tr} [\mathcal{G}_{\mathbf{k},\omega_n}^{\text{BdG}} \partial_\mu H_{\mathbf{k}}^+], \tag{A6}
\end{aligned}$$

where $\mathcal{G}_{\mathbf{k},\omega_n}^{\text{BdG}} = \mathcal{G}_{\mathbf{k},\mathbf{q},\omega_n}^{\text{BdG}}|_{\mathbf{q}=0}$. Here, we use the relationship $\partial_{\Delta_l(\mathbf{q})} F(\mathbf{q}) = 0$, in which $\Delta_l(\mathbf{q})$ denotes the \mathbf{k} -independent part of each component of the gap function, since the superconducting state is stable. Taking the sum of the Matsubara frequencies, we get the formula of the anapole moment as,

$$T_\mu = \frac{1}{2} \sum_{\mathbf{k}} \sum_a f(E_{a\mathbf{k}}) \langle \psi_{a\mathbf{k}} | \partial_\mu H_{\mathbf{k}}^+ | \psi_{a\mathbf{k}} \rangle. \tag{A7}$$

Appendix B: Anapole moment from GL theory

Here, we derive the formula of the anapole moment using the GL expansion. Since we focus on the superconducting state, we ignore the free-electron term and rewrite the free energy as,

$$\begin{aligned}
F_{\mathbf{q}} &= -\frac{1}{2\beta} \sum_{\mathbf{k}\omega_n} \text{Tr} \ln[\mathcal{G}_{\mathbf{k},\mathbf{q},\omega_n}^{\text{BdG}-1}], \\
&= -\frac{1}{2\beta} \sum_{\mathbf{k}\omega_n} \text{Tr} \left[\ln[1 - \mathcal{G}_{\mathbf{k},\mathbf{q},\omega_n} \mathcal{V}_{\mathbf{k}}] + \ln[\mathcal{G}_{\mathbf{k},\mathbf{q},\omega_n}^{-1}] \right], \\
&= \frac{1}{2\beta} \sum_{c=1}^{\infty} \sum_{\mathbf{k}\omega_n} \text{Tr} [\mathcal{G}_{\mathbf{k},\mathbf{q},\omega_n} \mathcal{V}_{\mathbf{k}} \mathcal{G}_{\mathbf{k},\mathbf{q},\omega_n} \mathcal{V}_{\mathbf{k}}]^c + \dots, \tag{B1}
\end{aligned}$$

where,

$$\mathcal{V}_{\mathbf{k}} = \begin{pmatrix} 0 & \Delta_{\mathbf{k}} \\ \Delta_{\mathbf{k}}^\dagger & 0 \end{pmatrix}, \tag{B2}$$

$$\mathcal{G}_{\mathbf{k},\mathbf{q},\omega_n}^{-1} = \mathcal{G}_{\mathbf{k},\mathbf{q},\omega_n}^{\text{BdG}-1} + \mathcal{V}_{\mathbf{k}}. \tag{B3}$$

Up to the second order of the superconducting order parameter, the free energy can be written as,

$$\begin{aligned}
F_{\mathbf{q}}^{\text{GL}} &= \frac{1}{2\beta} \sum_{\mathbf{k}\omega_n} \text{Tr} [\mathcal{G}_{\mathbf{k},\mathbf{q},\omega_n} \mathcal{V}_{\mathbf{k}} \mathcal{G}_{\mathbf{k},\mathbf{q},\omega_n} \mathcal{V}_{\mathbf{k}}], \\
&= \frac{1}{2\beta} \sum_{\mathbf{k}\omega_n} \text{tr} [\mathcal{G}_{\mathbf{k},\mathbf{q},\omega_n}^{\text{p}} \Delta_{\mathbf{k}} \mathcal{G}_{\mathbf{k},\mathbf{q},\omega_n}^{\text{h}} \Delta_{\mathbf{k}}^\dagger \\
&\quad + \mathcal{G}_{\mathbf{k},\mathbf{q},\omega_n}^{\text{h}} \Delta_{\mathbf{k}}^\dagger \mathcal{G}_{\mathbf{k},\mathbf{q},\omega_n}^{\text{p}} \Delta_{\mathbf{k}}], \\
&= \frac{1}{\beta} \sum_{\mathbf{k}\omega_n} \text{tr} [\mathcal{G}_{\mathbf{k},\mathbf{q},\omega_n}^{\text{p}} \Delta_{\mathbf{k}} \mathcal{G}_{\mathbf{k},\mathbf{q},\omega_n}^{\text{h}} \Delta_{\mathbf{k}}^\dagger], \tag{B4}
\end{aligned}$$

with $\mathcal{G}_{\mathbf{k},\mathbf{q},\omega_n}^{\text{p(h)-1}} = i\omega_n \mp H_{\mathbf{k}\pm\mathbf{q}}$. Then, expanding Eq. (B4) with respect to the \mathbf{q} up to the first order, we get,

$$\begin{aligned}
F_{\mathbf{q}}^{\text{GL}} &= \frac{1}{\beta} \sum_{\mathbf{k}\omega_n} \text{tr} [\partial_\mu \mathcal{G}_{\mathbf{k},\omega_n}^{\text{p}} \Delta_{\mathbf{k}} \mathcal{G}_{\mathbf{k},\omega_n}^{\text{h}} \Delta_{\mathbf{k}}^\dagger \\
&\quad - \mathcal{G}_{\mathbf{k},\omega_n}^{\text{p}} \Delta_{\mathbf{k}} \partial_\mu \mathcal{G}_{\mathbf{k},\omega_n}^{\text{h}} \Delta_{\mathbf{k}}^\dagger] q_\mu + \dots, \\
&= \frac{1}{\beta} \sum_{\mathbf{k}\omega_n} \text{tr} [\mathcal{G}_{\mathbf{k},\omega_n}^{\text{p}} \partial_\mu H_{\mathbf{k}} \mathcal{G}_{\mathbf{k},\omega_n}^{\text{p}} \Delta_{\mathbf{k}} \mathcal{G}_{\mathbf{k},\omega_n}^{\text{h}} \Delta_{\mathbf{k}}^\dagger \\
&\quad + \mathcal{G}_{\mathbf{k},\omega_n}^{\text{p}} \Delta_{\mathbf{k}} \mathcal{G}_{\mathbf{k},\omega_n}^{\text{h}} \partial_\mu H_{\mathbf{k}} \mathcal{G}_{\mathbf{k},\omega_n}^{\text{h}} \Delta_{\mathbf{k}}^\dagger] q_\mu + \dots. \tag{B5}
\end{aligned}$$

Here, we use $\partial_\mu \mathcal{G}_{\mathbf{k},\omega_n}^{\text{p(h)}} = (-) \mathcal{G}_{\mathbf{k},\omega_n}^{\text{p(h)}} \partial_\mu H_{\mathbf{k}} \mathcal{G}_{\mathbf{k},\omega_n}^{\text{p(h)}}$. Using the relationship, $\mathcal{G}_{\mathbf{k}\omega_n}^{\text{p}} = -\mathcal{G}_{\mathbf{k}-\omega_n}^{\text{h}}$, we obtain

$$\begin{aligned}
T_\mu^{\text{GL}} &= \frac{1}{\beta} \sum_{\mathbf{k}\omega_n} \text{tr} \left[\mathcal{G}_{\mathbf{k}\omega_n}^{\text{p}} \partial_\mu H_{\mathbf{k}} \mathcal{G}_{\mathbf{k}\omega_n}^{\text{p}} \Delta_{\mathbf{k}} \mathcal{G}_{\mathbf{k}\omega_n}^{\text{h}} \Delta_{\mathbf{k}}^\dagger \right. \\
&\quad \left. - \mathcal{G}_{\mathbf{k}\omega_n}^{\text{p}} \partial_\mu H_{\mathbf{k}} \mathcal{G}_{\mathbf{k}\omega_n}^{\text{p}} \Delta_{\mathbf{k}}^\dagger \mathcal{G}_{\mathbf{k}\omega_n}^{\text{h}} \Delta_{\mathbf{k}} \right]. \tag{B6}
\end{aligned}$$

In the remaining part of this section, we discuss the symmetry constraint on the anapole moment and simplify Eq. (B6). We assume that the normal state Hamiltonian is \mathcal{P} - and \mathcal{T} -symmetric, i.e., $H_{\mathbf{k}} \xrightarrow{\mathcal{P}} U_{\mathcal{P}} H_{-\mathbf{k}} U_{\mathcal{P}}^\dagger = H_{\mathbf{k}}$ and $H_{\mathbf{k}} \xrightarrow{\mathcal{T}} U_{\mathcal{T}} H_{-\mathbf{k}} U_{\mathcal{T}}^\dagger = H_{\mathbf{k}}$, where $U_{\mathcal{P}}$ is the unitary operator for the \mathcal{P} -symmetry. Here, we require that the \mathcal{T} operator commutes with the \mathcal{P} operator, i.e., $U_{\mathcal{T}} \mathcal{K} U_{\mathcal{P}} = U_{\mathcal{T}} U_{\mathcal{P}}^* \mathcal{K} = U_{\mathcal{P}} U_{\mathcal{T}} \mathcal{K}$ with complex conjugate operator \mathcal{K} and the \mathcal{P} operator is its own inverse, i.e., $U_{\mathcal{P}}^2 = \mathbf{1}$. In addition, the \mathcal{T} operator satisfies $U_{\mathcal{T}} \mathcal{K} U_{\mathcal{T}} \mathcal{K} = U_{\mathcal{T}} U_{\mathcal{T}}^* = -\mathbf{1}$, since we consider spinful electron systems.

Let us consider the \mathcal{T} -symmetry in the superconducting state. Under the \mathcal{T} operation, the pair potential follows $\Delta_{\mathbf{k}} U_{\mathcal{T}} \xrightarrow{\mathcal{T}} U_{\mathcal{T}} \Delta_{-\mathbf{k}}^* U_{\mathcal{T}}^T U_{\mathcal{T}}^T$. The fermionic anti-symmetry, $\Delta_{\mathbf{k}} U_{\mathcal{T}} = -U_{\mathcal{T}}^T \Delta_{-\mathbf{k}}^*$, leads to $U_{\mathcal{T}} \Delta_{-\mathbf{k}}^* U_{\mathcal{T}}^* U_{\mathcal{T}}^T = -\Delta_{\mathbf{k}}^\dagger U_{\mathcal{T}}^T = \Delta_{\mathbf{k}}^\dagger U_{\mathcal{T}}$ since $U_{\mathcal{T}} U_{\mathcal{T}}^* = -\mathbf{1}$ is satisfied, which means $\Delta_{\mathbf{k}} \xrightarrow{\mathcal{T}} \Delta_{\mathbf{k}}^\dagger$. As a result, when the pair potential is \mathcal{T} -symmetric, the first term of Eq. (B6) cancels out the second term, and therefore, the anapole moment vanishes.

Next, we consider the \mathcal{P} -symmetry. Since $U_{\mathcal{T}} U_{\mathcal{P}}^* = U_{\mathcal{P}} U_{\mathcal{T}}$ and $U_{\mathcal{P}}^2 = \mathbf{1}$ lead to $U_{\mathcal{P}} U_{\mathcal{T}} = U_{\mathcal{T}} U_{\mathcal{P}}^T$, the pair potential follows $\Delta_{\mathbf{k}} U_{\mathcal{T}} \xrightarrow{\mathcal{P}} U_{\mathcal{P}} \Delta_{-\mathbf{k}} U_{\mathcal{T}} U_{\mathcal{P}}^T = U_{\mathcal{P}} \Delta_{-\mathbf{k}} U_{\mathcal{P}}^\dagger U_{\mathcal{T}}$, which means $\Delta_{\mathbf{k}} \xrightarrow{\mathcal{P}} U_{\mathcal{P}}^\dagger \Delta_{-\mathbf{k}} U_{\mathcal{P}} = \Delta_{\mathbf{g}\mathbf{k}} - \Delta_{\mathbf{u}\mathbf{k}}$. Therefore, because of $U_{\mathcal{P}} \mathcal{G}_{\mathbf{k}\omega_n}^{\text{p(h)}} U_{\mathcal{P}}^\dagger = \mathcal{G}_{\mathbf{k}\omega_n}^{\text{p(h)}}$ and $U_{\mathcal{P}} \partial_{-\mu} H_{-\mathbf{k}} U_{\mathcal{P}}^\dagger = -\partial_\mu H_{\mathbf{k}}$ with $\partial_{-\mu} = \frac{\partial}{\partial(-k_\mu)}$, the \mathcal{P} -even part of the effective anapole moment,

$$\begin{aligned}
T_\mu^{\text{GL:even}} &= \frac{1}{\beta} \sum_{\mathbf{k}\omega_n} \text{tr} \left[\mathcal{G}_{\mathbf{k}\omega_n}^{\text{p}} \partial_\mu H_{\mathbf{k}} \mathcal{G}_{\mathbf{k}\omega_n}^{\text{p}} \Delta_{\mathbf{k}}^{\text{g}} \mathcal{G}_{\mathbf{k}\omega_n}^{\text{h}} \Delta_{\mathbf{k}}^{\text{g}\dagger} \right. \\
&\quad \left. - \mathcal{G}_{\mathbf{k}\omega_n}^{\text{p}} \partial_\mu H_{\mathbf{k}} \mathcal{G}_{\mathbf{k}\omega_n}^{\text{p}} \Delta_{\mathbf{k}}^{\text{u}\dagger} \mathcal{G}_{\mathbf{k}\omega_n}^{\text{h}} \Delta_{\mathbf{k}}^{\text{u}} \right] + (\mathbf{g} \leftrightarrow \mathbf{u}) \tag{B7}
\end{aligned}$$

vanishes due to the cancellation between \mathbf{k} and $-\mathbf{k}$. Thus, only the \mathcal{P} -odd and \mathcal{T} -odd part of the anapole moment becomes finite and we arrive at Eq. (10) in the main text.

Appendix C: Interband effect on anapole moment

Here, we show that at least two interband processes are needed for the anapole moment. We start from Eq. (11) based on the GL theory and consider the contribution from the purely intraband process, namely, the case $n = m = p$. Below, the \mathbf{k} dependence is omitted for simplicity. When $\chi_n = \chi_m = \chi_p$ is satisfied, the first and second terms of Eq. (11) obviously cancel out each other. Therefore, we consider the other cases.

First, when we fix the U(1) gauge of the Bloch wave function, we can define the relationship between the Kramers doublet through the \mathcal{PT} symmetry as $U_{\mathcal{PT}}|u_{n\uparrow}^*\rangle = |u_{n\downarrow}\rangle$ with $U_{\mathcal{PT}} = U_{\mathcal{P}}U_{\mathcal{T}}$; this leads to $-|u_{n\uparrow}\rangle = U_{\mathcal{PT}}|u_{n\downarrow}^*\rangle$ because of $U_{\mathcal{PT}}U_{\mathcal{PT}}^* = -1$. As a result, in the case of $\chi_n \neq \chi_m$, the velocity operator of the normal state vanishes as follows:

$$\begin{aligned} \langle u_{n\chi_n} | \partial H | u_{n\chi_m} \rangle &= (\langle u_{n\chi_m} | \partial H | u_{n\chi_n} \rangle)^* \\ &= \langle u_{n\chi_m}^* | \partial H^* | u_{n\chi_n}^* \rangle \\ &= \langle u_{n\chi_m}^* | U_{\mathcal{PT}}^\dagger U_{\mathcal{PT}} \partial H^* U_{\mathcal{PT}}^\dagger U_{\mathcal{PT}} | u_{n\chi_n}^* \rangle \\ &= -\langle u_{n\chi_n} | \partial H | u_{n\chi_m} \rangle \\ &= 0, \end{aligned} \quad (\text{C1})$$

since either χ_n or χ_m corresponds to the state \downarrow . Therefore, the contribution to Eq. (11) vanishes, and we have only to consider the rest case, $\chi_n = \chi_m \neq \chi_p$. In this case, contribution to Eq. (11) from each \mathbf{k} and ω_n can be written as,

$$\begin{aligned} \frac{1}{\beta} \sum_{n, \chi_n \neq \chi_p} C_{nmn}^{\text{GL}} \partial \epsilon_n (\langle u_{n\chi_n} | \Delta^g | u_{n\chi_p} \rangle \langle u_{n\chi_p} | \Delta^{u\dagger} | u_{n\chi_n} \rangle \\ + \langle u_{n\chi_p} | \Delta^g | u_{n\chi_n} \rangle \langle u_{n\chi_n} | \Delta^u | u_{n\chi_p} \rangle) - (g \leftrightarrow u). \end{aligned} \quad (\text{C2})$$

Because of $\Delta^g = \Delta^{g\dagger}$ and $\Delta^u = -\Delta^{u\dagger}$ except for the U(1)-gauge dependence of Cooper pairs, the first and second terms of Eq. (C2) cancel out each other. Thus, we found that the purely intraband process can not produce the anapole moment. This means that at least two interband effects are needed for the anapole superconductivity, as we discuss in Sec. III A.

Appendix D: Group velocity term, asymmetric BS, and BFS

In this section, we discuss the group velocity term of anapole moment. The following discussions are based on the general two-band model introduced in Sec. III B.

First, we show the close relationship between the group velocity term and asymmetric BS and elucidate the mechanism of the decay of the group velocity term in the low temperature region. Assuming $h_{0\mathbf{k}} \gg |\mathbf{h}_{\mathbf{k}}|$, we approximate the velocity operator in the BdG form,

$$\partial_\mu H_{\mathbf{k}}^+ = \partial_\mu h_{0\mathbf{k}} \mathbf{1}. \quad (\text{D1})$$

When the polar direction is denoted as μ , the anapole moment

is obtained from Eq. (4) as,

$$\begin{aligned} T_\mu &= \frac{1}{2} \sum_{\mathbf{k}} \sum_a f(E_{a\mathbf{k}}) \partial_\mu h_{0\mathbf{k}}, \\ &= \frac{1}{2} \sum_{\mathbf{k}(k_\mu > 0)} \sum_a (f(E_{a\mathbf{k}}) - f(E_{a-\mathbf{k}})) \partial_\mu h_{0\mathbf{k}}, \end{aligned} \quad (\text{D2})$$

which corresponds to the group velocity term since $\partial_\mu h_{0\mathbf{k}}$ is the group velocity. Thus, $f(E_{a\mathbf{k}}) - f(E_{a-\mathbf{k}})$, which represents the asymmetric structure of BS, induces the group velocity term. However, the Fermi distribution function is approximated by the step function, $f(E_{a\mathbf{k}}) \approx \theta(-E_{a\mathbf{k}})$, in the low temperature region, and therefore, $f(E_{a\mathbf{k}}) - f(E_{a-\mathbf{k}}) = 0$ at the zero temperature when $E_{a\mathbf{k}}$ and $E_{a-\mathbf{k}}$ have the same sign. Thus, the group velocity term vanishes at $T = 0$, unless the BFS are present.

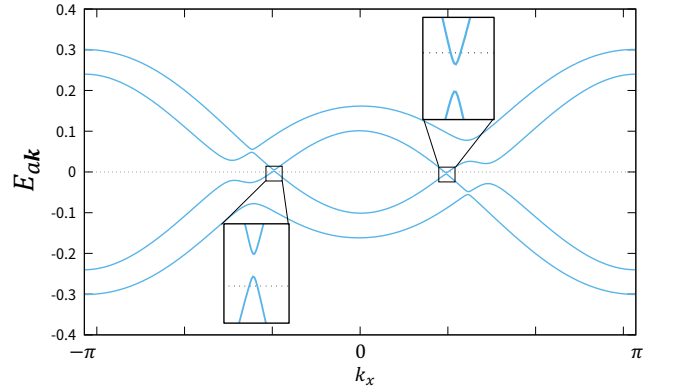


FIG. 5. BS on the line $(k_y, k_z) = (-0.862398, 0)$. We assume $\alpha = 0.04$ and the pair potential in Eqs. (D3) and (D4). Different from Fig. 3 in the main text, we set the center of mass momenta $\mathbf{q} = 0$. The inset illustrates the presence of the BFS.

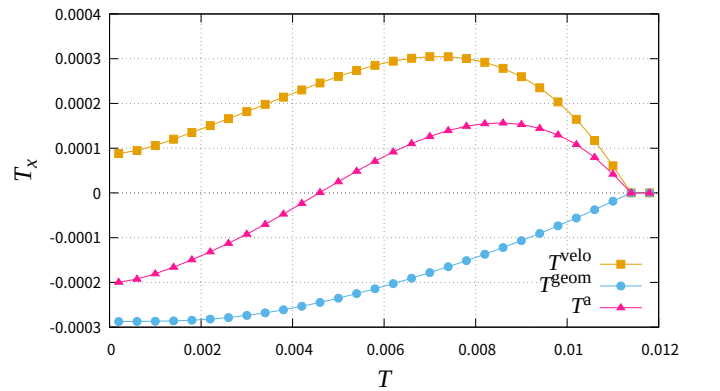


FIG. 6. The temperature dependence of the anapole moment for the pair potential Eqs. (D3) and (D4). All colors show the same quantities as in Fig. 1(a).

On the other hand, when the system has the BFS, $f(E_{a\mathbf{k}}) - f(E_{a-\mathbf{k}}) \neq 0$ even at $T = 0$. Thus, we expect that the group velocity term does not completely disappear at $T = 0$. To

verify this expectation, we consider the superconducting pair potential,

$$\Delta^g(T) = \frac{1}{2} \Delta_0(T) \phi_g^0 \sigma_0 \otimes \tau_0 + \Delta_0(T) d_{g,y}^z \sigma_y \otimes \tau_z, \quad (\text{D3})$$

$$\Delta^u(T) = i \Delta_0(T) d_{u,z}^0 \sigma_z \otimes \tau_0. \quad (\text{D4})$$

The difference from Eqs. (45) and (46) is only the factor $1/2$ in the first term of Eq. (D3). We show the BS for $\mathbf{q} = 0$ in Fig. 5. Different from the cases discussed in Sec. IV C, the BFS appear even for $\mathbf{q} = 0$. The temperature dependence of the anapole moment is shown in Fig. 6, and indeed, we see that the group velocity term is not completely suppressed at $T = 0$. Thus, the presence of the BFS at $\mathbf{q} = 0$ enhances the group velocity term, consistent with the above expectation. In this case, the anapole moment at $T = 0$ is not determined only by the geometric term. Even in this case, the sign change of the anapole moment can occur.

Appendix E: Superfluid weight and center of mass momenta of Cooper pairs

Here, we consider the variation of free energy with respect to the center of mass momentum of Cooper pairs q_μ in a direction along which the anapole moment T_μ is finite. Up to

the second order of q_μ , the superconducting free energy is expressed as,

$$F_{\mathbf{q}} = \frac{1}{2} D_{\mu\mu}^s q_\mu^2 + T_\mu q_\mu + F_0. \quad (\text{E1})$$

The superfluid density $D_{\mu\mu}^s$ is given by the formula⁶²,

$$\begin{aligned} D_{\mu\mu}^s &= \frac{1}{2} \sum_{\mathbf{k}} \sum_a f(E_{a\mathbf{k}}) \langle \psi_{a\mathbf{k}} | \partial_\mu \partial_\mu H_{\mathbf{k}}^- | \psi_{a\mathbf{k}} \rangle \\ &+ \frac{1}{2} \sum_{\mathbf{k}} \sum_{ab} \frac{f(E_{a\mathbf{k}}) - f(E_{b\mathbf{k}})}{E_{a\mathbf{k}} - E_{b\mathbf{k}}} \\ &\times \langle \psi_{a\mathbf{k}} | \partial_\mu H_{\mathbf{k}}^+ | \psi_{b\mathbf{k}} \rangle \langle \psi_{b\mathbf{k}} | \partial_\mu H_{\mathbf{k}}^+ | \psi_{a\mathbf{k}} \rangle, \end{aligned} \quad (\text{E2})$$

where,

$$H_{\mathbf{k}}^- = \begin{pmatrix} H_{\mathbf{k}} & 0 \\ 0 & -H_{\mathbf{k}} \end{pmatrix}. \quad (\text{E3})$$

The superconducting free energy is rewritten as,

$$F_{\mathbf{q}} = \frac{1}{2} D_{\mu\mu}^s (q_\mu + T_\mu / D_{\mu\mu}^s)^2 - T_\mu^2 / 2 D_{\mu\mu}^s + F_0. \quad (\text{E4})$$

Thus, the center of mass momentum q_c realizing the minimum free energy is estimated as $-T_\mu / D_{\mu\mu}^s$. This formula is valid when q_c is small.

* kitamura.taisei.67m@st.kyoto-u.ac.jp

- ¹ E. Bauer and M. Sigrist, eds., [Non-Centrosymmetric Superconductors: Introduction and Overview](#) (Springer, Berlin, Heidelberg, 2012).
- ² M. Smidman, M. B. Salamon, H. Q. Yuan, and D. F. Agterberg, [Rep. Prog. Phys.](#) **80**, 036501 (2017).
- ³ I. A. Sergienko, [Phys. Rev. B](#) **69**, 174502 (2004).
- ⁴ Y. Wang and L. Fu, [Phys. Rev. Lett.](#) **119**, 187003 (2017).
- ⁵ W. Yang, C. Xu, and C. Wu, [Phys. Rev. Research](#) **2**, 042047 (2020).
- ⁶ P. Goswami and B. Roy, [Phys. Rev. B](#) **90**, 041301 (2014).
- ⁷ K. Shiozaki and S. Fujimoto, [Phys. Rev. B](#) **89**, 054506 (2014).
- ⁸ B. Roy, [Phys. Rev. B](#) **101**, 220506 (2020).
- ⁹ S. Ryu, J. E. Moore, and A. W. W. Ludwig, [Phys. Rev. B](#) **85**, 045104 (2012).
- ¹⁰ X.-L. Qi, E. Witten, and S.-C. Zhang, [Phys. Rev. B](#) **87**, 134519 (2013).
- ¹¹ T. Scaffidi, (2020), [arXiv:2007.13769 \[cond-mat.supr-con\]](#).
- ¹² S. Ran, C. Eckberg, Q.-P. Ding, Y. Furukawa, T. Metz, S. R. Saha, I.-L. Liu, M. Zic, H. Kim, J. Paglione, and N. P. Butch, [Science](#) **365**, 684 (2019).
- ¹³ D. Aoki, J.-P. Brison, J. Flouquet, K. Ishida, G. Knebel, Y. Tokunaga, and Y. Yanase, [Journal of Physics: Condensed Matter](#) **34**, 243002 (2022).
- ¹⁴ J. Ishizuka and Y. Yanase, [Phys. Rev. B](#) **103**, 094504 (2021).
- ¹⁵ D. Braithwaite, M. Vališka, G. Knebel, G. Lapertot, J.-P. Brison, A. Pourret, M. E. Zhitomirsky, J. Flouquet, F. Honda, and D. Aoki, [Communications Physics](#) **2**, 1 (2019).
- ¹⁶ S. Ran, H. Kim, I.-L. Liu, S. R. Saha, I. Hayes, T. Metz, Y. S. Eo, J. Paglione, and N. P. Butch, [Phys. Rev. B](#) **101**, 140503 (2020).

- ¹⁷ W.-C. Lin, D. J. Campbell, S. Ran, I.-L. Liu, H. Kim, A. H. Nevidomskyy, D. Graf, N. P. Butch, and J. Paglione, [npj Quantum Materials](#) **5**, 1 (2020).
- ¹⁸ G. Knebel, M. Kimata, M. Vališka, F. Honda, D. Li, D. Braithwaite, G. Lapertot, W. Knafo, A. Pourret, Y. J. Sato, Y. Shimizu, T. Kihara, J.-P. Brison, J. Flouquet, and D. Aoki, [J. Phys. Soc. Jpn.](#) **89**, 053707 (2020).
- ¹⁹ D. Aoki, F. Honda, G. Knebel, D. Braithwaite, A. Nakamura, D. Li, Y. Homma, Y. Shimizu, Y. J. Sato, J.-P. Brison, and J. Flouquet, [Journal of the Physical Society of Japan](#) **89**, 053705 (2020).
- ²⁰ S. M. Thomas, F. B. Santos, M. H. Christensen, T. Asaba, F. Ronning, J. D. Thompson, E. D. Bauer, R. M. Fernandes, G. Fabbris, and P. F. S. Rosa, [Sci. Adv.](#) **6** (2020).
- ²¹ S. M. Thomas, C. Stevens, F. B. Santos, S. S. Fender, E. D. Bauer, F. Ronning, J. D. Thompson, A. Huxley, and P. F. S. Rosa, [Phys. Rev. B](#) **104**, 224501 (2021).
- ²² C. Duan, K. Sasmal, M. B. Maple, A. Podlesnyak, J.-X. Zhu, Q. Si, and P. Dai, [Phys. Rev. Lett.](#) **125**, 237003 (2020).
- ²³ M. Vališka, W. Knafo, G. Knebel, G. Lapertot, D. Aoki, and D. Braithwaite, [Phys. Rev. B](#) **104**, 214507 (2021).
- ²⁴ N. P. Butch, S. Ran, S. R. Saha, P. M. Neves, M. P. Zic, J. Paglione, S. Gladchenko, Q. Ye, and J. A. Rodriguez-Rivera, [npj Quantum Materials](#) **7**, 1 (2022).
- ²⁵ C. Duan, R. E. Baumbach, A. Podlesnyak, Y. Deng, C. Moir, A. J. Breindel, M. B. Maple, E. M. Nica, Q. Si, and P. Dai, [Nature](#) **600**, 636 (2021).
- ²⁶ S. Raymond, W. Knafo, G. Knebel, K. Kaneko, J.-P. Brison, J. Flouquet, D. Aoki, and G. Lapertot, [J. Phys. Soc. Jpn.](#) **90**, 113706 (2021).
- ²⁷ D. V. Ambika, Q.-P. Ding, K. Rana, C. E. Frank, E. L. Green, S. Ran, N. P. Butch, and Y. Furukawa, [Phys. Rev. B](#) **105**, L220403 (2022).

- (2022).
- ²⁸ S. Kanasugi and Y. Yanase, *Communications Physics* **5**, 1 (2022).
- ²⁹ K. I. Wysokiński, J. F. Annett, and B. L. Györfy, *Phys. Rev. Lett.* **108**, 077004 (2012).
- ³⁰ E. Taylor and C. Kallin, *Phys. Rev. Lett.* **108**, 157001 (2012).
- ³¹ M. Gradhand, K. I. Wysokinski, J. F. Annett, and B. L. Györfy, *Phys. Rev. B* **88**, 094504 (2013).
- ³² D. F. Agterberg, P. M. R. Brydon, and C. Timm, *Phys. Rev. Lett.* **118**, 127001 (2017).
- ³³ P. M. R. Brydon, D. F. Agterberg, H. Menke, and C. Timm, *Phys. Rev. B* **98**, 224509 (2018).
- ³⁴ N. A. Spaldin, M. Fiebig, and M. Mostovoy, *J. Phys. Condens. Matter* **20**, 434203 (2008).
- ³⁵ J. Jeong, Y. Sidis, A. Louat, V. Brouet, and P. Bourges, *Nat. Commun.* **8**, 15119 (2017).
- ³⁶ H. Murayama, K. Ishida, R. Kurihara, T. Ono, Y. Sato, Y. Kasahara, H. Watanabe, Y. Yanase, G. Cao, Y. Mizukami, T. Shibauchi, Y. Matsuda, and S. Kasahara, *Phys. Rev. X* **11**, 011021 (2021).
- ³⁷ H. Watanabe and Y. Yanase, *Phys. Rev. X* **11**, 011001 (2021).
- ³⁸ J. Ahn, G.-Y. Guo, and N. Nagaosa, *Phys. Rev. X* **10**, 041041 (2020).
- ³⁹ V. V. Flambaum, I. B. Khriplovich, and O. P. Sushkov, *Phys. Lett. B* **146**, 367 (1984).
- ⁴⁰ P. Fulde and R. A. Ferrell, *Phys. Rev.* **135**, A550 (1964).
- ⁴¹ A. I. Larkin and Y. N. Ovchinnikov, *Zh.Éksp. Teor. Fiz.* **47**, 1136 (1964), [*Sov. Phys. JETP* **20**, 762 (1965)].
- ⁴² M. Chazono, H. Watanabe, and Y. Yanase, *Phys. Rev. B* **105**, 024509 (2022).
- ⁴³ M. Chazono, S. Kanasugi, T. Kitamura, and Y. Yanase, (2022), [arXiv:2212.13102 \[cond-mat.supr-con\]](https://arxiv.org/abs/2212.13102).
- ⁴⁴ R. P. Kaur, D. F. Agterberg, and M. Sigrist, *Phys. Rev. Lett.* **94**, 137002 (2005).
- ⁴⁵ The Josephson effect is proposed for the detection of the phase modulation in the helical superconductivity⁴⁴. We consider that this method is also useful for observing the phase modulation in the anapole superconductivity.
- ⁴⁶ Y. Matsuda and H. Shimahara, *Journal of the Physical Society of Japan* **76**, 051005 (2007).
- ⁴⁷ N. Marzari and D. Vanderbilt, *Phys. Rev. B* **56**, 12847 (1997).
- ⁴⁸ R. Resta, *Eur. Phys. J. B* **79**, 121 (2011).
- ⁴⁹ Y. Gao, S. A. Yang, and Q. Niu, *Phys. Rev. Lett.* **112**, 166601 (2014).
- ⁵⁰ Y. Gao and D. Xiao, *Phys. Rev. Lett.* **122**, 227402 (2019).
- ⁵¹ M. F. Lapa and T. L. Hughes, *Phys. Rev. B* **99**, 121111 (2019).
- ⁵² A. Daido, A. Shitade, and Y. Yanase, *Phys. Rev. B* **102**, 235149 (2020).
- ⁵³ A. Julku, G. M. Bruun, and P. Törmä, *Phys. Rev. B* **104**, 144507 (2021).
- ⁵⁴ A. Julku, G. M. Bruun, and P. Törmä, *Phys. Rev. Lett.* **127**, 170404 (2021).
- ⁵⁵ D. D. Solnyshkov, C. Leblanc, L. Bessonart, A. Nalitov, J. Ren, Q. Liao, F. Li, and G. Malpuech, *Phys. Rev. B* **103**, 125302 (2021).
- ⁵⁶ Q. Liao, C. Leblanc, J. Ren, F. Li, Y. Li, D. Solnyshkov, G. Malpuech, J. Yao, and H. Fu, *Phys. Rev. Lett.* **127**, 107402 (2021).
- ⁵⁷ J.-W. Rhim, K. Kim, and B.-J. Yang, *Nature* **584**, 59 (2020).
- ⁵⁸ T. Kitamura, J. Ishizuka, A. Daido, and Y. Yanase, *Phys. Rev. B* **103**, 245114 (2021).
- ⁵⁹ S. Peotta and P. Törmä, *Nature Communications* **6**, 8944 (2015).
- ⁶⁰ L. Liang, T. I. Vanhala, S. Peotta, T. Siro, A. Harju, and P. Törmä, *Phys. Rev. B* **95**, 024515 (2017).
- ⁶¹ P. Törmä, S. Peotta, and B. A. Bernevig, *Nature Reviews Physics* **4**, 528 (2022).
- ⁶² T. Kitamura, T. Yamashita, J. Ishizuka, A. Daido, and Y. Yanase, *Phys. Rev. Research* **4**, 023232 (2022).
- ⁶³ M. D. E. Denys and P. M. R. Brydon, *Phys. Rev. B* **103**, 094503 (2021).
- ⁶⁴ P. M. R. Brydon, D. S. L. Abergel, D. F. Agterberg, and V. M. Yakovenko, *Phys. Rev. X* **9**, 031025 (2019).
- ⁶⁵ A. Ramires and M. Sigrist, *Phys. Rev. B* **94**, 104501 (2016).
- ⁶⁶ A. Ramires, D. F. Agterberg, and M. Sigrist, *Phys. Rev. B* **98**, 024501 (2018).
- ⁶⁷ S. Khim, J. F. Landaeta, J. Banda, N. Bannor, M. Brando, P. M. R. Brydon, D. Hafner, R. Kuchler, R. Cardoso-Gil, U. Stockert, A. P. Mackenzie, D. F. Agterberg, C. Geibel, and E. Hassinger, *Science* **373**, 1012 (2021).
- ⁶⁸ M. H. Fischer, M. Sigrist, D. F. Agterberg, and Y. Yanase, *Annu. Rev. Condens. Matter Phys.* (2023).
- ⁶⁹ The two-orbital model with orbitals of same (opposite) parity is given by the permutation, $(\tau_x, \tau_y, \tau_z) \rightarrow (\tau_z(y), \tau_x(z), \tau_y(x))$.
- ⁷⁰ H. Watanabe and Y. Yanase, *Phys. Rev. B* **98**, 245129 (2018).
- ⁷¹ A. Rosuel, C. Marcenat, G. Knebel, T. Klein, A. Pourret, N. Marquardt, Q. Niu, S. Rousseau, A. Demuer, G. Seyfarth, G. Lapertot, D. Aoki, D. Braithwaite, J. Flouquet, and J.-P. Brison, (2022), [arXiv:2205.04524 \[cond-mat.supr-con\]](https://arxiv.org/abs/2205.04524).
- ⁷² H. Sakai, Y. Tokiwa, P. Opletal, M. Kimata, S. Awaji, T. Sasaki, D. Aoki, S. Kambe, Y. Tokunaga, and Y. Haga, (2022), [arXiv:2210.05909 \[cond-mat.supr-con\]](https://arxiv.org/abs/2210.05909).
- ⁷³ Considering that the group velocity term is also the first-order of $\partial\xi$, the sign of the $\partial\xi$, which is determined by structure of the band dispersion, is also crucial for the group velocity term.
- ⁷⁴ J. Wang, Y. Che, L. Zhang, and Q. Chen, *Phys. Rev. B* **97**, 134513 (2018).
- ⁷⁵ P. Zdybel, M. Homenda, A. Chlebicki, and P. Jakubczyk, *Phys. Rev. A* **104**, 063317 (2021).
- ⁷⁶ H. Watanabe, A. Daido, and Y. Yanase, *Phys. Rev. B* **105**, 024308 (2022).
- ⁷⁷ H. Watanabe, A. Daido, and Y. Yanase, *Phys. Rev. B* **105**, L100504 (2022).
- ⁷⁸ A. Daido, Y. Ikeda, and Y. Yanase, *Phys. Rev. Lett.* **128**, 037001 (2022).
- ⁷⁹ L. Jiao, S. Howard, S. Ran, Z. Wang, J. O. Rodriguez, M. Sigrist, Z. Wang, N. P. Butch, and V. Madhavan, *Nature* **579**, 523 (2020).
- ⁸⁰ I. M. Hayes, D. S. Wei, T. Metz, J. Zhang, Y. S. Eo, S. Ran, S. R. Saha, J. Collini, N. P. Butch, D. F. Agterberg, A. Kapitulnik, and J. Paglione, *Science* **373**, 797 (2021).